REVIEW

Check for updates

Metal–organic frameworks for petroleum-based platform compound separations

Xiaolai Zhang,[a] Xiaokang Wang, [ID][b] Fei Gao,[b] Yue Chen,[c] Hongyan Liu,[b] Pengfei Zhou,[c] Zixi Kang,[b] Yutong Wang [ID]*[b] and Weidong Fan [ID]*[b]

The advancement of separation technology is not only conducive to lowering energy consumption, but also opens an avenue to obtain the world's key resources. Metal–organic frameworks (MOFs), a novel type of porous materials, have unique advantages in separation and purification compared with traditional adsorbents and separation technologies, especially in the separation of petroleum-based platform compounds, owing to their advantages of easy structure regulation and functionalization. Significant advancements have been achieved in the separation of binary component petroleum-based platform compounds based on MOFs. However, industrial gas mixtures often exist in multiple components. In contrast to the rapid development of binary mixture separations, the separation of ternary and even multi-component mixtures is much more difficult and rarely achieved with a single material. This review briefly introduces the adsorptive separation technology and its mechanism based on MOFs. Next, recent advances in MOFs for the separation of multiple-component petroleum-based platform compounds ($C_2H_2/C_2H_4/C_2H_6/CO_2$, $C_3H_4/C_3H_6/C_3H_8$, butane/butene/isobutene/1,3-butadiene, *trans*-2-pentene/1-pentene/isoprene, *n*-hexane/2-methylpentane/3-methylpentane/2,2-dimethylbutane/2,3-dimethylbutane, *o*-xylene/*m*-xylene/*p*-xylene/ethylbenzene, *etc.*) are presented to guide more complex chemical separation processes. Furthermore, inherent obstacles and future development prospects from academia to eventual industrial implementation are presented. Based on adsorptive separation technology, we are committed to exploring an alternative separation route that is energy-efficient and environmentally friendly and strives to achieve the high-efficiency separation of multi-component petroleum-based platform compounds.

1 Introduction

Separation and purification of chemical feedstocks consumes approximately 15% of the global energy.[1,2] As human demand for chemicals increases year by year, this energy demand is likely to triple by 2050. For example, the separation and purification of ethylene and propylene consume 0.3% of global energy.[3] Such huge energy demand has forced mankind to seek a more economical and efficient method for the purification and separation of mixed gas.

Taking the separation and purification of C_2H_4 as an example, in the past, to obtain C_2H_4 with a purity of not less than 99.9% from industrial gas mixtures, it was necessary to remove C_2H_2 from a mixed gas *via* catalytic hydrogenation or solvent extraction and to remove C_2H_6 *via* cryogenic distillation.[4,5]

Since the kinetic radius and quadrupole moment of C_2H_4 are between those of C_2H_2 and C_2H_6, the separation of these ternary mixtures through physical adsorption faces enormous difficulties.[6–8] In particular, when there are CO_2 and water vapors in a mixed gas, separating and obtaining polymer-grade C_2H_4 from the mixed gas require more complicated process steps, which further increases the energy consumption cost.[9–11] Therefore, the development of economical and efficient mixed gas purification and separation technology has great strategic value to produce high-purity C_2H_4 and even more chemicals.

Adsorptive separation technology has gradually become a research focus owing to its high efficiency, energy-saving feature, and environmental friendliness.[12] In this regard, the development of novel adsorbent materials, such as carbon-based adsorbents, zeolites, and metal–organic frameworks (MOFs), has become an important frontier research field owing to their excellent properties of suitable specific surface area, pore size, and stability.[13–15] The clearly tunable crystalline structure of MOFs makes them convenient platforms to investigate structure–activity relationships, which enable them to show enormous advantages in both basic research and practical applications.[16–19]

[a] School of Chemistry and Chemical Engineering, Shandong University, Jinan, 250014, China

[b] State Key Laboratory of Heavy Oil Processing, School of Materials Science and Engineering, China University of Petroleum (East China), Qingdao, Shandong 266580, China. E-mail: wdfan@upc.edu.cn

[c] State Key Lab of Fluorinated Functional Membrane Materials, Zibo, 256401, China

Two-component separation, including gas–liquid separation, whether based on MOF adsorptive separation or membrane separation, has made significant progress.[20–24] For example, in 2016, two studies on the separation of light hydrocarbons were simultaneously reported in Science. Chen et al.[25] succeeded in separating the C_2H_4/C_2H_2 mixture utilizing the strong host–guest interaction between the strongly basic SiF_6^{2-} and the more acidic C_2H_2 molecule. Eddaoudi et al.[26] realized the molecular sieving of C_3H_6/C_3H_8 by replacing the SiF_6^{2-} node with a larger size $NbOF_5^{2-}$ node and controlled the pore size of MOF at 4.75 Å. These two researches opened new directions for the study of MOFs in the field of adsorption and separation. Afterwards, Zhang et al.[27] achieved the purification of 1,3-butadiene by controlling the configurational change of C4 hydrocarbons in MOF channels. By tuning the perturbation of the pore wall to control the diffusion of gas molecules in porous materials, Kitagawa et al.[28] realized the separation of C_2H_4/C_2H_6 exploiting the variation in gas molecule diffusion kinetics. With the in-depth study of hydrocarbon separation, there are also many important reviews summarizing the separation progress, which have guided the follow-up research. For example, Eddaoudi et al.[29] summarized the application of microporous MOFs for gas/vapour separation. Xing et al.[12] summarized MOF adsorbents and membranes for hydrocarbon separation. Zaworotko et al.[30] summarized the crystal engineering of porous MOFs to enable the separation of C2 hydrocarbons. Li et al.[31] summarized the opportunities and critical factors of porous MOFs for industrial light olefins separation. However, most of the petrochemical processes involved are multi-component separations, for instance, $C_2H_2/C_2H_4/C_2H_6/CO_2$, $C_3H_4/C_3H_6/C_3H_8$, butane/butene/isobutene/1,3-butadiene, trans-2-pentene/1-pentene/isoprene, and n-hexane/2-methylpentane/3-methylpentane/2,2-dimethylbutane/2,3-dimethylbutane, o-xylene/m-xylene/p-xylene/ethylbenzene (Table 1). The physical and chemical properties of these molecules with the same carbon number are very similar, making separation extremely difficult (Fig. 1). The study of multi-component hydrocarbons separation can better guide the industrial separation process. However, in contrast to the rapid development of binary mixture separations, the separation of ternary and even multi-component mixtures is much more difficult and rarely achieved with a single material.

Herein, a brief introduction to the novel adsorptive separation technology and mechanism based on MOFs is given. Then, from the perspective of structural design and regulation of MOFs, the separation progress of related multi-component mixtures in petroleum-based platform compounds with increasing carbon number is summarized (Fig. 2), aiming to explore the efficient and low-energy separation of multi-component petroleum-based platform compounds.

2 Adsorptive separation technology and mechanism

The most recently reported methods for the separation and purification of petroleum-based platform compounds using MOFs focus on adsorptive separation technology,[32] which is

Table 1 Physical characteristics for selected hydrocarbon molecules

Adsorbate	Kinetic diameter (Å)	Molecular dimensions (Å³)	Boiling point (K)	Polarizability ($\times 10^{-25}$ cm³)
CO_2	3.3	3.18 × 3.33 × 5.36	194.7	29.11
Methane (CH_4)	3.758	3.829 × 4.101 × 3.942	111.6	25.93
Acetylene (C_2H_2)	3.3	3.32 × 3.34 × 5.7	189.3	33.3–39.3
Ethylene (C_2H_4)	4.163	3.28 × 4.18 × 4.84	169.4	42.52
Ethane (C_2H_6)	4.443	3.809 × 4.079 × 4.821	184.4	44.3–44.7
Propyne (C_3H_4)	4.76	6.5 × 4.0 × 4.2	250	—
Propylene (C_3H_6)	4.678	6.5 × 4.0 × 3.8	225.4	62.6
Propane (C_3H_8)	4.3–5.118	6.61 × 4.52 × 4.02	231.1	62.9–63.7
n-Butane (n-C_4H_{10})	4.7	4.2 × 4.6 × 4.7	272.6	82.0
Iso-butane (i-C_4H_{10})	5.3	4.3 × 6.0 × 6.8	261.4	81.4–82.9
trans-2-Butene (trans-2-C_4H_8)	4.31	3.5 × 4.6 × 7.0	274	81.8
cis-2-Butene (cis-2-C_4H_8)	4.94	3.6 × 4.9 × 6.2	277	82
1,3-Butadiene (1,3-C_4H_6)	4.31	2.7 × 4.6 × 7.3	268.3	86.4
1-Butene (n-C_4H_8)	4.46	3.5 × 4.5 × 7.4	266.9	79.7–85.2
Iso-butene (i-C_4H_8)	4.84	3.6 × 5.2 × 6.0	266.2	80
1-Pentene	—	8.8 × 5.0 × 5.1	303	99.8
Isoprene	—	7.7 × 6.0 × 4.0	308	97.1
trans-2-Pentene	—	8.7 × 4.6 × 4.9	310	—
n-Hexane (nHEX)	4.3	10.344 × 4.536 × 4.014	341	119
2-Methylpentane (2MP)	5.5	9.2 × 6.4 × 5.3	333	—
3-Methylpentane (3MP)	5.5	9.3 × 6.2 × 5.2	336	—
2,2-Dimethylbutane (22DMB)	6.2	8 × 6.7 × 5.9	323	—
2,3-Dimethylbutane (23DMP)	5.8	7.8 × 6.7 × 5.3	331	—
Benzene (Bz)	5.349–5.85	6.628 × 7.337 × 3.277	353.3	100–107.4
Cyclohexane (Cy)	6.0	5.0–6.6–7.2	353.9	108.7–110
Toluene	5.25	6.625 × 4.012 × 8.252	383.8	118–123
Ethylbenzene (EB)	5.8	6.625 × 5.285 × 9.361	409.3	142
Styrene (ST)	5.3	6.7 × 3.3 × 9.7	418.3	—
p-Xylene (PX)	5.8	6.618 × 3.81 × 9.146	411.5	137–149
o-Xylene (OX)	6.8	7.269 × 3.834 × 7.826	417.5	141–149
m-Xylene (MX)	6.8	8.994 × 3.949 × 7.315	412	142
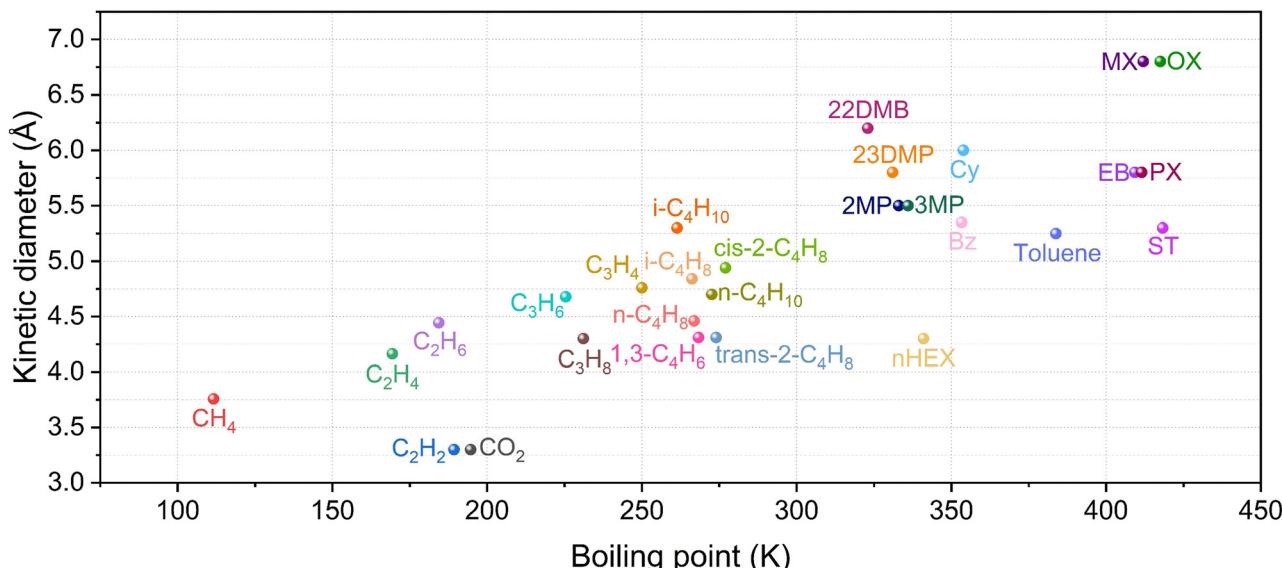
Fig. 1 Kinetic diameter–boiling point diagram of hydrocarbon compounds. The closer they are, the harder it is to separate them.

Fig. 2 Schematic diagram of metal–organic frameworks for the separation of multi-component petroleum compounds based on adsorptive separation technology.

an operation process in which a porous solid substance is contacted with a mixed component system (gas or liquid), and one or more components in the system are selectively attached to the solid surface, thereby realizing the separation of specific components.

In the petroleum-based platform compounds separation by MOFs, the mechanism based on thermodynamic adsorption is the most common. It refers to the separation of two or more components due to the difference in affinity between the adsorbates and MOFs, which is an important factor in determining the separation effect. This is the separation of thermodynamic balance. This interaction usually represents the adsorption heat of the gas molecule at zero coverage. The intensity of the interaction depends on the surface nature of MOF adsorbents and the molecular characteristics of the adsorbates, including but not limited to molecular polarization, dipole moment and quadrupole moment. Therefore, introducing strong binding sites is an effective approach to enhance the binding strength. This strategy typically modified polar groups on the surface, or open-metal sites (OMSs), to selectively enhance the interaction of guest molecules. OMSs can form metal–π effects with unsaturated carbon bonds, thereby enhancing the affinity with olefin and separating olefins from their mixtures with alkanes. For example, M-MOF-74 (M = Fe, Co, Ni, Cu, Zn, and Mg) may be the most studied isomorphic series with high OMSs density among the numerous MOF structures reported in the past two decades. Although M-MOF-74 cannot realize the sieving effect due to their large pores (11 Å), their abundant OMSs on the pore surface preferentially interact with unsaturated hydrocarbons rather than saturated counterparts. Therefore, they exhibit potential application for the separation of C_2H_4/C_2H_6 and C_3H_6/C_3H_8. Among them, Fe-MOF-74 features square pyramid shaped Fe^{2+} cations arranged on hexagonal channels, and each cation has an unsaturated site pointing towards the channel.[33] Fe-MOF-74 exhibits strong affinity for unsaturated hydrocarbons, with Fe–C distances ranging from 2.42(2) to 2.60(2) Å. Therefore, Fe-MOF-74 has been demonstrated not only in the separation of C_2H_4/C_2H_6 and C_3H_6/C_3H_8 mixtures but also in the separation of $CH_4/C_2H_6/C_2H_4/C_2H_2$ equimolar four component mixtures. The mechanism by which OMS was introduced on the pore surface of MOFs to enhance the separation effect of olefin/alkane is clear and robust. This is a practical and feasible strategy. However, most OMSs are prone to loss or

decomposition under humid conditions, and OMSs can interact with alkanes through polarization; thus, the olefin/alkanes selectivity is limited.

The thermodynamic adsorptive separation mechanism is achieved through the difference in the supramolecular force of each component, while the kinetic diffusion separation mechanism is achieved through different diffusion rates of each component in the framework. Due to the difference in the kinetic diffusion rates, a shorter time is needed for some components to enter the pores and achieve adsorption equilibrium. For the separation process dominated by kinetic effects, it is necessary to control the pore size of the adsorbents between the dynamic diameters of the two gas molecules to be separated. The differences in pore size, pore shape, and physical/chemical properties of MOFs will result in significant differences in the kinetic diffusion rates of various gas molecules in the pores. For gas molecules with higher mobility, the preferential occupation of the pore space and the completion of separation process before other components reach adsorption equilibrium lead to the higher separation selectivity. Relatively speaking, MOFs based on the kinetic diffusion separation mechanisms are rare. Unlike the macroscopic size effect, the kinetic diffusion at the microscopic level cannot simply consider the kinetic diameter of the guest molecule and the size of the bottleneck but also consider whether the electrostatic potential of the guest molecule matches the electrostatic potential at the bottleneck.[34]

Based on the kinetic diffusion separation mechanism, we can take full advantage of the controllable and adjustable pore size and pore shape of MOFs to further narrow the bottleneck restricting the diffusion of gas molecules between the kinetic diameters of olefins and alkanes to maximize the selectivity of olefins/alkanes through the separation mechanism of the molecular sieve. Due to the ultra-high adsorption selectivity, molecular sieve MOFs have great application prospects in the separation of petroleum-based platform compounds. In addition to molecular sieves based on size, the potential for regulating the surface chemistry of MOFs can also be regarded as molecular sieves based on interaction to preferentially adsorb molecules exhibiting stronger host–guest interactions, rather than necessarily small-sized molecules. This usually involves specific active sites, such as Lewis base/acid sites, π-complex sites, and other polar groups. However, the currently reported molecular sieve MOFs usually place a bottleneck in the channel, i.e., the bottleneck is part of the channel. Although this design can selectively allow the target molecules to enter the channel, it inevitably increases the mass transfer resistance during the diffusion of guest molecules, which may lead to extended time and increased energy consumption during the adsorption and desorption process.

In addition to the structural adjustment characteristics of MOFs such as pore size, pore shape, and active site, another significant feature of MOFs is that the framework may be very flexible. Flexible MOFs produce rich and diverse structural responses and dynamic behaviors to external stimuli to achieve the precise regulation of target molecular adsorption.

Flexibility is a rather interesting feature distinguishing some MOFs from traditional porous materials, such as zeolite and carbon materials. After removing the solvent filled in the pores, flexible MOFs typically shrink to smaller pores or even non-porous states, which typically exhibit different reactions for various gas molecules and experience reversible framework transformation under external stimuli, such as pressure and temperature. When gas pressure increases, one typical framework flexibility is gate opening. Specifically, different adsorbate molecules lead to various gate opening pressures, and even the final stretchable state after complete adsorption can be different. Therefore, for MOFs with framework flexibility, the pore size and pore shape can be precisely controlled through external stimuli to optimize the separation performance of specific gas mixtures. The flexibility of MOFs can be simply divided into overall framework flexibility and partial flexibility. The most representative of the overall framework flexibility is the respiration effect, such as MIL-53, in which the ligand connected to the metal atom can be distorted when adsorbing guest molecules, causing their pores to transition between closed and open configurations, and the adsorption curve was significantly stepped.[35] The most representative of the partial framework flexibility is the dynamic gating effect. When the concentration of guest molecules reaches a certain level or is stimulated by other external factors, the host–guest force causes the rotation or distortion of local single bonds or planes, thereby selectively adsorbing guest molecules or controlling the diffusion of guest molecules in the pore. The separation mechanism based on the dynamic gating effect has gained increasing attention in the last few years because of its significant separation effect on petroleum-based platform compounds.[36]

3 Separation of gases from petroleum-based platform compounds

3.1 Separation of C2 mixtures

C_2H_4 is a common feedstock for the synthesis of polymers and valuable organic compounds in the chemical industry.[37,38] The steam cracking of naphtha and C_2H_6 dehydrogenation are the primary methods for obtaining C_2H_4, which produce impurities such as C_2H_2 and C_2H_6.[39] Due to their comparable molecular sizes and boiling points, separating C2 mixtures is a challenging processes.[40] Currently, the industrial separation of C_2H_6 and C_2H_4 mainly adopts thermally-driven high-pressure cryogenic distillation technology, and the process requires low temperatures (180–258 K) and high pressures (5–28 bar), which is both extremely energy-intensive and expensive.[9,41] Therefore, it is urgent to develop separation technologies with higher energy efficiency, lower energy consumption, and simpler separation process. With fast adsorption kinetics and low regeneration temperature, physical adsorption is expected to greatly reduce the energy consumption of petroleum-based platform compounds separation.

Many experiments have confirmed that MOFs as adsorbents can effectively separate C_2H_2/C_2H_4,[42–44] C_2H_4/C_2H_6,[38,45–47] and

C_2H_4/C_3H_6.[17,48] Current studies indicate that the purification of C_2H_4 using MOFs involves three strategies: (1) the precise control over the pore size to achieve the desired molecular sieving effect; (2) selectively increasing the interaction between MOF and hydrocarbons; and (3) synergistic sorbent separation technology (SSST) because MOFs capable of simultaneously adsorbing C_2H_6 and C_2H_2 for C_2H_4 purification are still very rare. The limitation can be compensated by connecting multiple ultra-microporous MOFs with different molecular recognition orientations connected in series in a single adsorption column,[4] such as two different MOFs in series, that are respectively optimized for C_2H_2/C_2H_4 and C_2H_4/C_2H_6 mixtures. However, this synergistic sorbent separation technology is limited by the stacking sequence and gas mass transfer between adsorbents, making it difficult to achieve industrial-scale separation. Therefore, it is very meaningful to develop novel MOF adsorbents to achieve the one-step purification of polymer-grade C_2H_4 (purity >99.99%). The rapid progress of crystal engineering and reticular chemistry of MOFs provides guidance for the separation of multiple components, aiming to develop MOFs that meet purity targets and concomitantly have the highest productivity of purified C_2H_4 per kg of adsorbent packed in the bed.

3.1.1 Separation of $C_2H_2/C_2H_4/C_2H_6$. Compared with the separation of two-component mixed gas, the separation of three gases is more difficult, and there are few examples of separation that can be achieved with only one material in the current research.

In response to this problem, Chen *et al.*[49] used a novel hexanuclear manganese ($[Mn_6(\mu_3\text{-}O)_2(CH_3COO)_3]^{6+}$) cluster as a secondary building unit, which was connected with mixed organic ligands to fabricate a series of strong polar isostructural MOFs with dual cage-like cavities, namely, NPU-1/2/3, which successfully achieved the one-step separation and preparation of C_2H_4 from an equimolar mixture of $C_2H_2/C_2H_4/C_2H_6$ (Fig. 3). The double cage-like structure in NPU-1/2/3 can be fine-tuned according to the size of the cage to achieve the selective separation of C_2H_4. The results of the breakthrough experiments demonstrate that NPU-1 can produce C_2H_4 with a purity of over 99.9% from equimolar $C_2H_2/C_2H_4/C_2H_6$ mixture. Theoretical calculations show that the preferential adsorption of C_2H_6 and C_2H_2 by NPU-1 to C_2H_4 is for the following reason: (a) in one cage, the electronegative carboxylate O atom and C_2H_2 molecule have strong hydrogen-bonding interactions; (b) in the other cage, there are multiple non-covalent interactions between ligands in the framework and C_2H_6 molecules.

We[50] also reported a pore segmentation strategy based on a MOF-525 with a stable **ftw** topology to modify the pore environment (Fig. 4). Two novel MOFs (UPC-612 and UPC-613) were prepared by introducing cyclopentadienyl cobalt, which enhanced the host–guest interaction and achieved one-step purification of C_2H_4 from the C2 hydrocarbon mixtures. The introduction of cyclopentadiene cobalt has two advantages: one is selectively increasing the interaction between the framework and two impurities (C_2H_2 and C_2H_6), and the other is dividing the cubic cage into two parts, forming a spherical-like force

surface, which further increases the interaction between the gas and the framework. The selective and differential adsorption of C_2H_2 and C_2H_6 enables the one-step purification of C_2H_4 in a large proportion of three-component mixed gas. Meanwhile, the density functional theory (DFT) calculation demonstrated that the introduction of cyclopentadienyl cobalt enhances the interaction of the MOF framework with C_2H_2 and C_2H_6. C_2H_2 and C_2H_6 are preferentially adsorbed by the framework, which is beneficial for the purification of C_2H_4. The breakthrough experiments demonstrated that the material can generate polymer-grade C_2H_4 from an equimolar $C_2H_2/C_2H_4/C_2H_6$ mixture with high yield and low energy cost. The modification method proposed in this work provides a new strategy for realizing the one-step purification of C_2H_4 in three-component C2 gas mixture. In addition, we reported a Co-MOF (UPC-66), which exhibits an adaptive pore structure under external stimuli.[51] The activated UPC-66-a possesses the unique ability to exhibit dynamic changes in the pore size in response to pressure, temperature, and guest molecules. UPC-66-a can not only purify ethylene from C_2H_2/C_2H_4 and C_2H_6/C_2H_4 mixture but also realize one-step purification to obtain polymer-grade ethylene from a three-component mixture of $C_2H_2/C_2H_4/C_2H_6$. The single-crystal structures of MOF loaded with gas molecules accurately determine the adsorption sites of gas molecules in the MOF channels and their interactions with the framework. This work provides meaningful guidance for the multi-component separations with flexible materials that adapt and change according to the external environment.

Furthermore, other research groups have also made good contributions to the separation of $C_2H_2/C_2H_4/C_2H_6$. Hu *et al.*[52] reported a structurally stable Mg-MOF (NUM-9) for the separation of C_2H_6 and C_2H_2 from C_2H_4 feed gas. At 100 kPa and 313 K, NUM-9 can well separate C_2H_4 in binary C_2H_6/C_2H_4 and C_2H_2/C_2H_4 mixtures and ternary $C_2H_6/C_2H_2/C_2H_4$ mixtures. The separation mechanism of NUM-9 is the different host–guest interaction, which is revealed by the Grand Canonical Monte Carlo (GCMC) simulations. Lu *et al.*[53] reported a microporous MOF (TJT-100) with high acid–base and thermal stability. Uncoordinated carboxylic acid oxygen atoms and coordinated water molecules can form weak electrostatic interactions with C–H bonds of C_2H_6 and C_2H_2 on the microporous surface, which does not happen to C_2H_4. This enables the MOF adsorbent to efficiently purify C_2H_4 (purity >99.997%) in a ternary $C_2H_2/C_2H_4/C_2H_6$ (0.5 : 99 : 0.5) mixture. Chen *et al.*[54] reported a Th-MOF (Azole-Th-1) with an **fcu** topology based on Th_6 cluster and tetrazolyl linkers (Fig. 5). This unique structure is linked *via* a highly chemically stable N,O-donor ligand. Azole-Th-1 can well separate C_2H_4 (purity over 99.9%) from binary C_2H_6/C_2H_4 (1 : 9) and ternary $C_2H_6/C_2H_2/C_2H_4$ (9 : 1 : 90) mixtures at 100 kPa and 298 K, and the corresponding productivities can reach 1.13 and 1.34 mmol g^{-1}, respectively. DFT calculations reveal that the separation mechanism is the strong van der Waals interaction between C_2H_6 and the Azole-Th-1 framework. Recently, they[55] used the stable, low-cost and scalable material MOF-303 as the research object, proposed a strategy to build a negative electrostatic pore environment, and achieved an
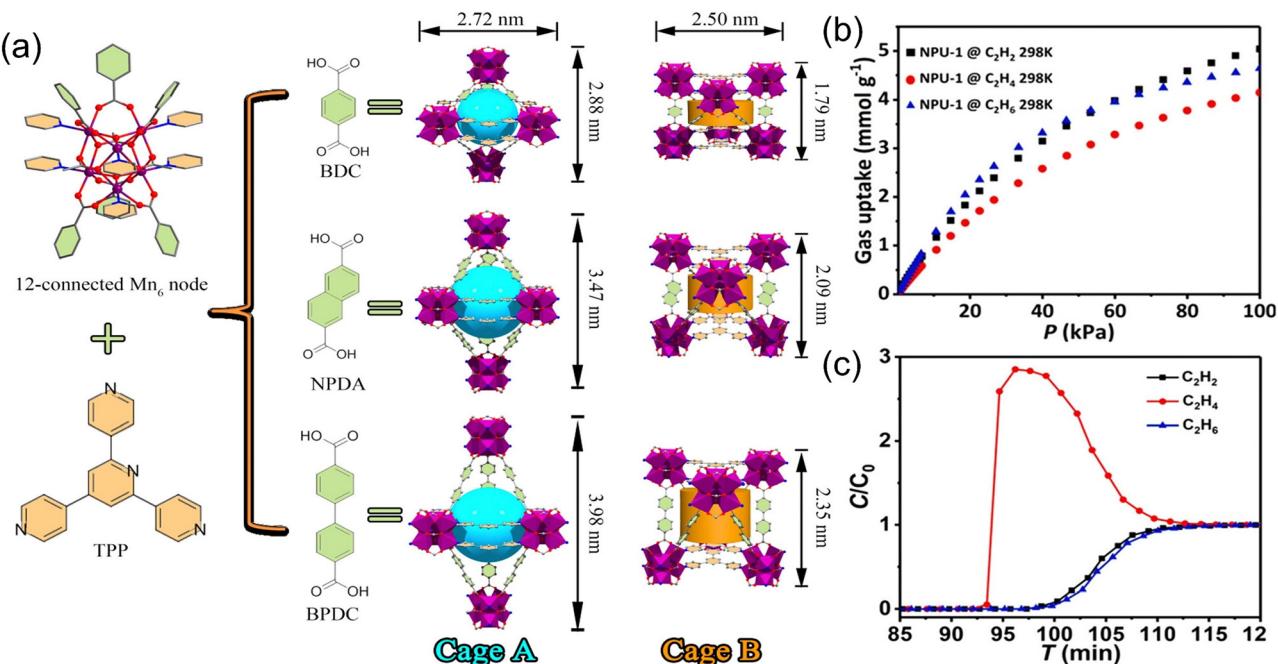
Fig. 3 (a) A series of isostructural MOFs (NPU-1/2/3) with double caged cavities. (b) C2 gas sorption isotherms of NPU-1. (c) Experimental breakthrough curves of $C_2H_2/C_2H_4/C_2H_6$ separation (1:1:1) based on NPU-1 at 298 K. Reproduced with permission from ref. 49. Copyright © 2021, American Chemical Society.
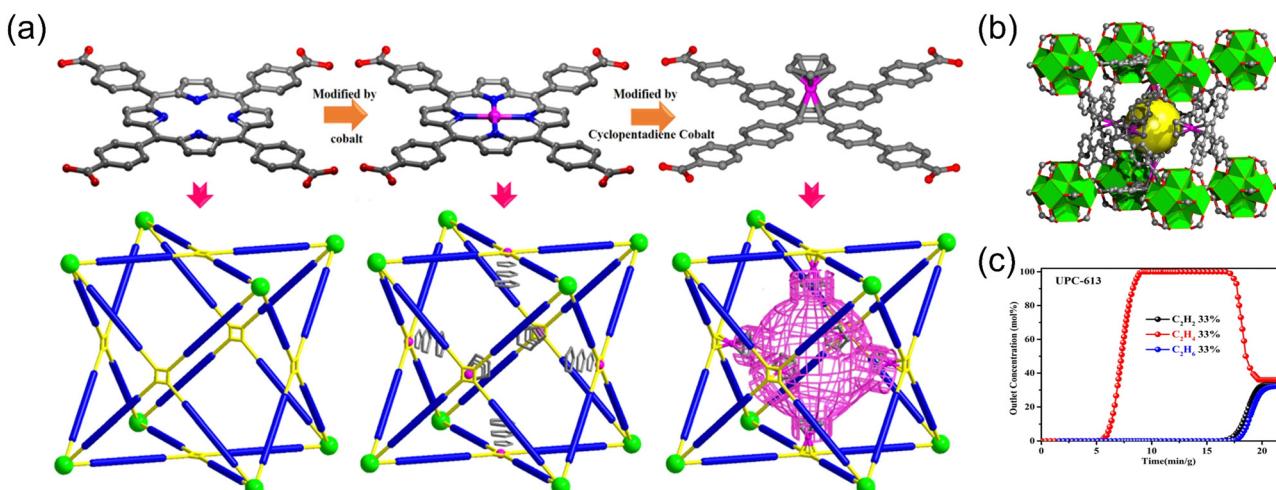

Fig. 4 (a) The progressive process of linker modification based on **ftw** topology platform in Zr-MOFs. (b) Three-dimensional view of unit cubic cages. (c) Experimental column breakthrough curves for $C_2H_6/C_2H_4/C_2H_2$ (33/33/33) mixtures absorber bed packed with UPC-613. Reproduced with permission from ref. 50. Copyright © 2020, Wiley-VCH GmbH.

efficient one-step separation of $C_2H_2/C_2H_6/C_2H_4$ ternary mixtures. Su *et al.*[56] used a dynamic ligand insertion strategy to construct a series of multiple MOFs (LIFM-XYY-1–8). By installing different functional ligands, the nanospace of the intrinsic MOF (LIFM-28/PCN-700) can be precisely controlled, such as reducing the pore size, increasing the pore volume, and functionalizing the pore surface, thereby realizing efficient purification of C_2H_4 in three-component C2 hydrocarbons,

which provides a new idea for the development of multiple MOFs for adsorption and separation.

In addition to achieving selective separation through different interaction forces between the framework and petroleum-based platform compounds, tuning of the pore size can also be incorporated. Recently, Li *et al.*[39] first reported the introduction of Lewis base sites on the MOF framework with C_2H_6-selective adsorption capacity, which realizing the one-step purification
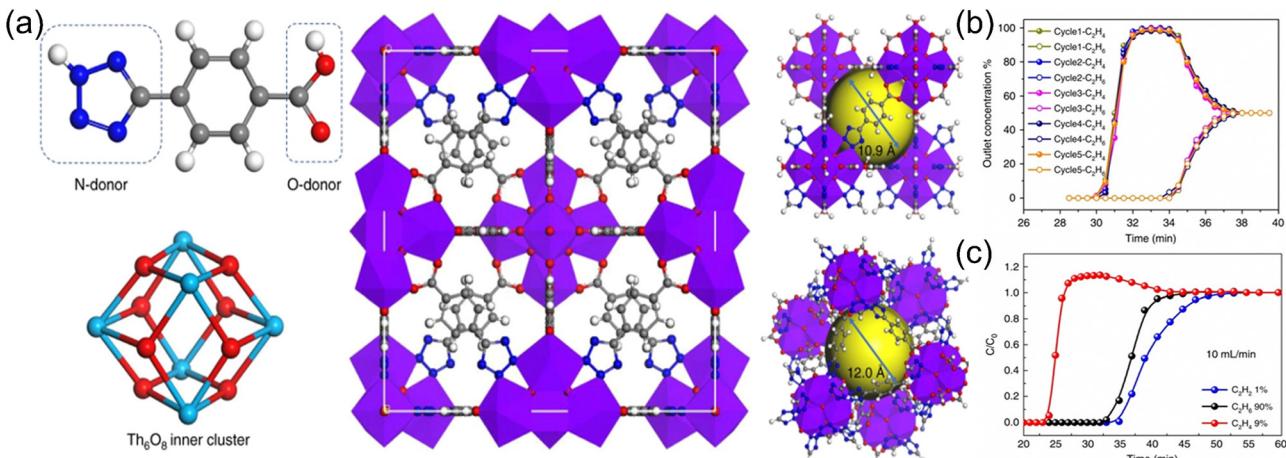
Fig. 5 (a) A Th-MOF (Azole-Th-1) based on Th_6 secondary building unites and tetrazolyl groups. (b) C_2H_6/C_2H_4 (50/50, v/v) binary mixture separation for five cycles. (c) $C_2H_6/C_2H_4/C_2H_2$ (90/9/1, v/v/v) ternary mixture separation. Reproduced with permission from ref. 54. Copyright © 2020, Springer Nature Publishing AG.

of C_2H_4 to polymer-grade purity from a ternary mixture (Fig. 6). The assembly of amino groups in the UiO-67 framework structure reduced the larger pore structure into a smaller cage-like pocket, thus improving the confinement environment of the pore. In addition, the amino group also could serve as a binding site to improve the preferential adsorption of C_2H_6 and C_2H_2. Amino-modified UiO-67-$(NH_2)_2$ achieves extremely high C_2H_6 and C_2H_2 adsorption capacity and achieves excellent C_2H_2/C_2H_4, C_2H_6/C_2H_4 adsorption selectivity, superior to all reported C_2H_2- and C_2H_6-selective materials. *In situ* infrared characterization techniques coupled with theoretical calculations reveal that the overall stronger multipoint van der Waals interactions with C_2H_6 and C_2H_2 is due to the appropriate pore confinement environment and aminated surface. The $C_2H_4/C_2H_6/C_2H_2$ separation performance was investigated

under dry and wet conditions, respectively, and it was verified that a C_2H_4 yield of 0.55 mmol g^{-1} was achieved under mild conditions.

Recently, Zhang *et al.*[57] proposed a strategy to couple host–guest interactions and molecular shape matching for the efficient removal of C_2H_2 and C_2H_6 from $C_2H_2/C_2H_4/C_2H_6$ using a heterocyclic ultra-microporous MOF with spindle-shaped molecular cages. The material contains a high density of uncoordinated carbonyl oxygen atoms and polar nitrogen-containing heterocycles, which can preferentially bind C_2H_2 and C_2H_6 through hydrogen bonding and C–H···π interactions, respectively. At the same time, based on the shape-matching effect, C_2H_6 as a stereo molecule can more fully contact with the surrounding heterocycles than C_2H_4, while C_2H_2 as a linear molecule can form strong hydrogen bonds with the oxygen
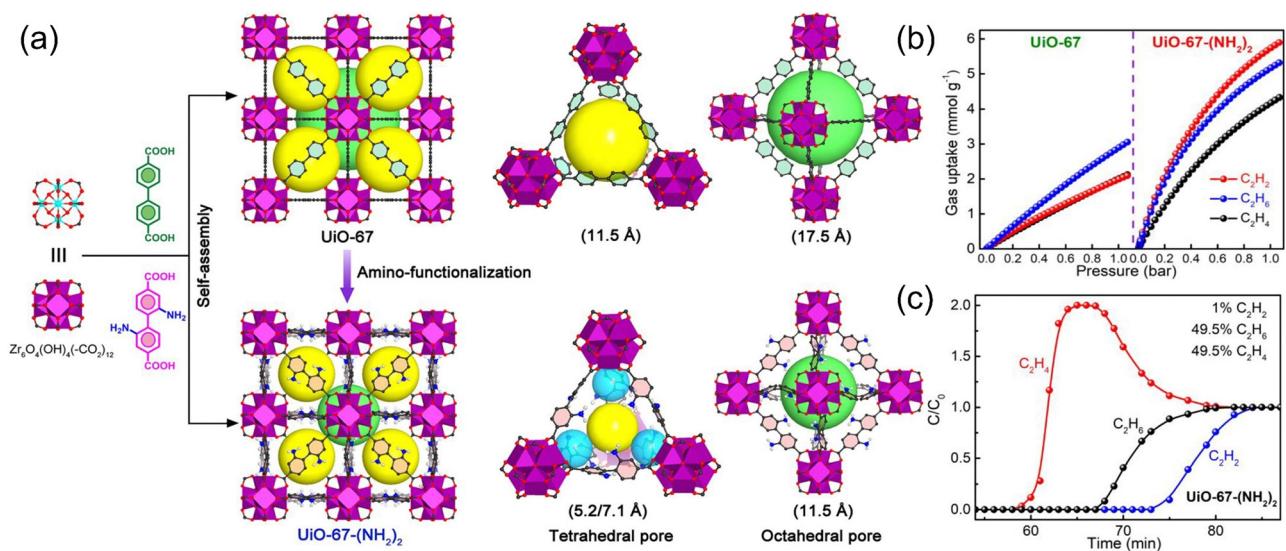
Fig. 6 (a) Comparison of the crystal structures, tetrahedral cages, and octahedral cages of UiO-67 and UiO-67-$(NH_2)_2$. (b) Gas adsorption isotherms of UiO-67 (left) and UiO-67-$(NH_2)_2$ (right) at 296 K. (c) Experimental column breakthrough curves of UiO-67-$(NH_2)_2$ for 1/49.5/49.5 ternary mixtures under ambient conditions. Reproduced with permission from ref. 36. Copyright © 2022, American Chemical Society.

atoms located at the corners of the molecular cage, effectively promoting the recognition process of C2 molecules. This study presents an efficient approach for the separation and purification of structurally similar multi-component low-carbon hydrocarbons. Hou *et al.*[58] adopt the strategy of "combining non-polar pores and active sites" and customized MOFs with a special pore environment. The MOF has a priority adsorption function for C_2H_2 and C_2H_6 in C2 hydrocarbons, which realizes the production of highly-pure C_2H_4 from the mixed gas of C_2H_6/C_2H_4/C_2H_2.

In-depth comparative analysis will find it impossible to conclude which of the four different breakthroughs in Fig. 3c, 4c, 5c and 6c, or Zhang *et al.*[57] offers the best separation performance. In each case, the inlet flow rates of gas mixtures, the gas compositions, and the mass of MOFs packed in the tube are not the same. Thus, it is impossible to judge which MOF offers the best prospects. In this context, it is worth mentioning that the proper way to compare breakthrough experiments is to use the modified time parameter (as explained by Krishna[59]).

$$\frac{(Q_0 = \text{inlet flow rate mL min}^{-1}) \times (\text{time in min})}{(\text{g MOF packed in tube})} = \frac{Q_0 t}{m_{ads}}$$
$$= \text{mL g}^{-1}$$

In future scientific articles, it would be helpful to be able to compare the original published data according to the modification time $\frac{Q_0 t}{m_{ads}}$.

3.1.2   Separation of C_2H_4/C_2H_2/CO_2. During the oxidative coupling of CH_4 to C_2H_4, C_2H_2 and CO_2 cannot be avoided as by-products. At this time, it will involve the problem of removing C_2H_2 and CO_2 from the C_2H_2/CO_2/C_2H_4 ternary mixture. Due to the close polarity and size of these three gas molecules, it is extremely challenging to purify C_2H_4 from the C_2H_2/CO_2/C_2H_4 ternary mixture in one step. So far, only a small number of MOF materials can achieve this goal because rigid MOFs with C_2H_4 adsorption sites also simultaneously adsorb CO_2, and these materials still have problems like low adsorption capacity and high operating environment requirements. Consequently, there remains a need for ideal materials that can realize the one-step purification of C_2H_4 from the C_2H_2/CO_2/C_2H_4 ternary mixture.

Flexible MOFs with controllable gate opening pressure provide new opportunities for C_2H_2/CO_2/C_2H_4 separation.[60–64] Chen *et al.*[65] proposed a separation strategy by adjusting the gate opening pressure of a flexible MOF (NTU-65, Fig. 7). The opening pressure of CO_2, C_2H_2, and C_2H_4 can be realized
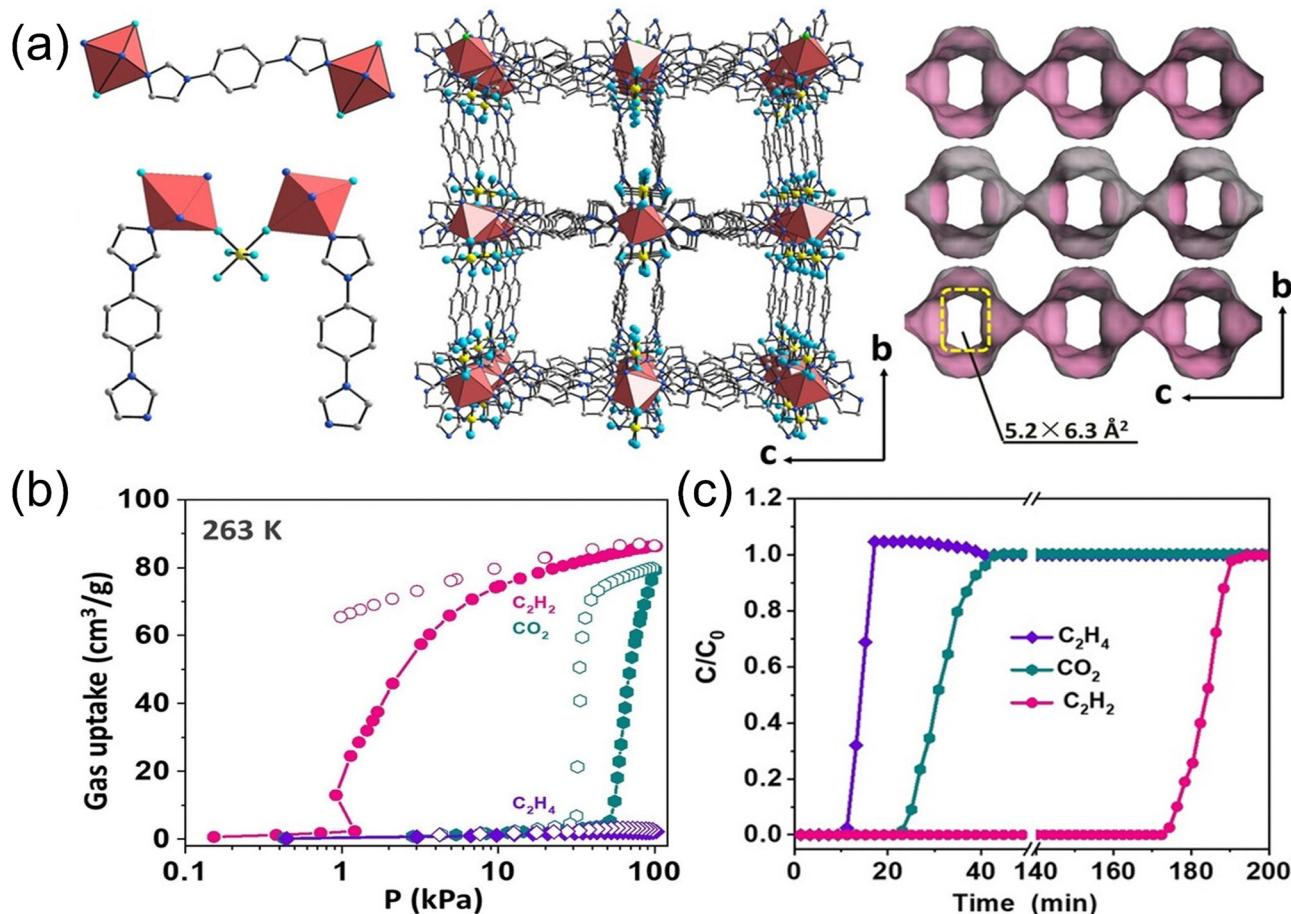
Fig. 7   (a) Structure and channel of NTU-65. (b) C_2H_2, C_2H_4, and CO_2 adsorption isotherms of NTU-65 at 263 K. (c) Breakthrough curves of NTU-65 at 263 K. Reproduced with permission from ref. 65. Copyright © 2020, Wiley-VCH GmbH.

through temperature adjustment to efficiently screen and separate the ternary mixed gas. At low temperature, the desolvated MOF framework will simultaneously adsorb three gases. As the temperature rises, the gate opening pressure increases, and the frame will adsorb CO_2 and C_2H_2 that are smaller in size or have a stronger force with the frame, resulting in the desired high-purity gas. At high temperature, only C_2H_2 can cause a phase change and be adsorbed, and the separation is not complete. At the optimal temperature (263 K), NTU-65 adsorbed a lot of CO_2 and C_2H_2 by opening the gate, while the adsorption of C_2H_4 was negligible. Breakthrough experiments demonstrate that NTU-65 can simultaneously capture CO_2 and C_2H_2 to generate high-purity C_2H_4. In addition, they use the post-synthetic method of single crystal to single crystal in the boiling alkaline solution to synthesize MOF (NTU-67) with a trap-and-flow channel.[66] Based on the shape and size-dependent dynamic screening effect, NTU-67 can obtain record C_2H_4 productivity (121.5 mL g^{-1}, >99.95%) from the C_2H_2/ CO_2/C_2H_4 (1/9/90) mixture.

Optimizing the pore environment of the existing structure is another effective strategy. Pyrazine-linked hybrid ultra-microporous materials (HUMs) with ultra-small pore (<7 Å) has higher selectivity for CO_2 than the adsorption properties of other small molecules, which can be used for the capture of trace CO_2 as well as hydrocarbon molecules. By modifying the crystal structure of HUM, specifically by substituting metal and inorganic structures, the second generation of HUM was developed. In view of this, Zaworotko et al.[67] reported a HUM formed by linking two aminopyrazines with the structure MFSIX-17-Ni (M = Si, Ti, 17 = aminopyrazine, Fig. 8). The modified material

with the amine group did not exhibit higher CO_2 affinity and capture performance than the bulk HUMs but showed higher C_2H_2 affinity. At the same time, MFSIX-17-Ni first realized the single-step physical adsorption of CO_2, obtaining the polymer level C_2H_4 (>99.95%) in the ternary equal ratio mixture (C_2H_4/ C_2H_2/CO_2). By comparing MFSIX-17-Ni and SIFSIX-3-Zn, this high-efficiency C_2H_2 adsorption capacity was attributed to the difference in the bonding structure.

Recently, Zhang et al.[68] reported a GeF_6^{2-} anion intercalated MOF (ZNU-6), with large pores ($\sim$8.5 Å) connected by narrow channels ($\sim$4 Å), which can be used as a benchmark material for the one-step purification of C_2H_4 from C_2H_2/CO_2/C_2H_4 mixtures. ZNU-6 exhibited excellent adsorption capacities (8.06/4.76 mmol g^{-1}) for C_2H_2 and CO_2 and high ideal adsorbed solution theory (IAST) selectivity for C_2H_2/C_2H_4 (1/99, S = 14.3) and CO_2/C_2H_4 (1/99, S = 7.8). The zero-load adsorption enthalpy (Q_{st}) of C_2H_2, CO_2, and C_2H_4 was calculated to be 37.2, 37.1, and 29.0 kJ mol^{-1}, respectively, which once again showed that the affinity of ZNU-6 for C_2H_2 and CO_2 was better than that of C_2H_4. In addition, the moderate Q_{st} is beneficial to the regeneration of materials. The breakthrough experiment proves that ZNU-6 has excellent dynamic separation performance for both two-component and three-component gas mixtures. The breakthrough test was carried out on ZNU-6 using C_2H_2/CO_2/C_2H_4 (1/1/98, 1/5/94, 1/9/90) mixtures with different composition ratios, and 64.42, 21.37, 13.81 mol kg^{-1} of polymer grade C_2H_4 can be obtained respectively. In addition, ZNU-6 has excellent cycle stability and water stability and has great application potential under industrial conditions. DFT calculations prove that there are two adsorption sites for the three gases in
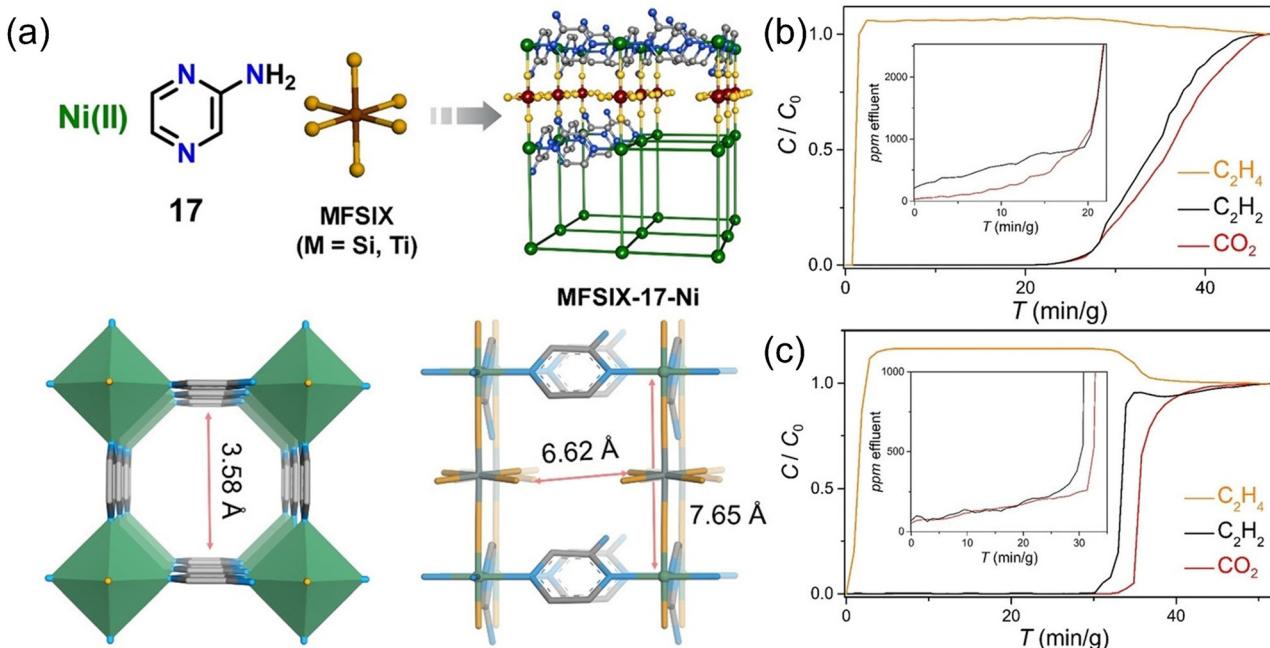
Fig. 8 (a) Structure and channel diagram of TIFSIX-17-Ni. Ambient temperature (298 K) and pressure (1 bar) experimental dynamic column breakthrough curves for C_2H_4/C_2H_2/CO_2 (1:1:1, v/v/v) ratio by a sorbent bed filled with (b) SIFSIX-17-Ni and (c) TIFSIX-17-Ni. Reproduced with permission from ref. 67. Copyright © 2021, Wiley-VCH GmbH.

ZNU-6, which are in the narrow channel pores and the cage-like pores, and the binding energies of the three gases in the channels are all higher than that of the cage-like pores, indicating that the gas is preferentially adsorbed on the channel pores. In addition, in the channel pore, the order of binding energy of the three gases is $C_2H_2 > CO_2 > C_2H_4$. The analysis of the *in situ* gas-loaded single crystal further reveals the interaction sites between the guest molecules and the framework, and the results show that the framework mainly forms the interaction force with the guest molecules through two kinds of adsorption sites, namely, macro cavity and staggered aisle. This research emphasizes the importance of tuning both the pore structure and pore chemistry of porous materials to construct multiple synergistic functions for gas separation.

3.1.3 Separation of $C_2H_4/C_2H_6/CO_2$. C_2H_4 is majorly derived from the cracking of C_2H_6 or naphtha, and C_2H_6 as a by-product of petroleum refining is also separated from natural gas (CH$_4$: 70–96%, C_2H_6: 1–4%, and CO_2: 0–8%) on an industrial scale. In industry, C_2H_6 and C_2H_4 are separated by cryogenic high-pressure distillation with huge energy consumption. Developing a separation method at room temperature is vital for saving energy. It is very meaningful to separate the mixed gas through a fixed bed to achieve low energy consumption and high purity separation. The unsaturated carbon–carbon bonds of C_2H_4 can be combined with metal ions to achieve C_2H_4/C_2H_6 separation. Compared with other porous materials, MOFs possess gas separation potential because of their designable pore environments including exposed metal sites. Compared with C_2H_4-selective adsorbents, the C_2H_6-selective approach can save about 40% energy consumption on pressure swing adsorption (PSA) technology. Therefore, a more ideal separation method is to develop C_2H_6 adsorbents. Considering the difference in the positively and negatively charged moieties of these gas molecules, it is still possible to design MOFs with optimized pore size/shape and surface to generate stronger electrostatic binding to C_2H_6 using polar functional groups. Chen et al.[9] synthesized MAF-49 using H$_2$batz as the organic

ligand: the nitrogen atom acts as a hydrogen bond acceptor, and the methylene group acts as a dipole repulsive group. The hydrogen bond between MAF-49 and C_2H_6 is the strongest, and the binding energies of MAF-49 with C_2H_4, C_2H_6, and CO_2 are 56.7, 45.5, and 41.3 kJ mol^{-1}, respectively. Thus, it can preferentially adsorb C_2H_6 and realize three-component $C_2H_4/C_2H_6/CO_2$ separation.

3.1.4 Separation of $C_2H_2/C_2H_4/C_2H_6/CO_2$. The four gases, C_2H_4, C_2H_2, C_2H_6 and CO_2, often "go hand in hand" in the production of chemical raw materials. To achieve the one-step separation and preparation of C_2H_4, a specific "porous MOF material" must achieve the simultaneous removal of the other three gases from the above-mentioned mixtures. This principle is very simple but it is difficult to put into practice due to the quite similar physical characteristics of C2 gases.

Chen et al.[4] utilized the synergy between three high-performance ultra-microporous MOFs to realize the one-step separation and preparation of high-purity C_2H_4 in a four-component hybrid system (Fig. 9). This study found that by effectively connecting three MOF materials in a single adsorption column, C_2H_2, C_2H_6, and CO_2 could be removed sequentially and efficiently using synergistic sorbent separation technology. Thus, a one-step separation and collection of high-purity C_2H_4 ($>99.9\%$) is achieved at the end of the adsorption column. That is, TIFSIX-2-Cu-i, Zn-atz-ipa, and SIFSIX-3-Ni were sequentially used to separate C_2H_2, C_2H_6, and trace CO_2 in the mixed gas, respectively. This physical adsorptive separation process can be carried out under normal temperature conditions, which can greatly decrease the energy consumption in the C_2H_4 separation process. However, this synergistic sorbent separation technology is limited by the stacking order and gas mass transfer between adsorbents, and the purification efficiency of C_2H_4 is very low, making it difficult to achieve industrial-scale separation.

At the same time, this achievement explained the microscopic interaction mechanism between four gas molecules and three MOF materials in the system from the molecular scale by
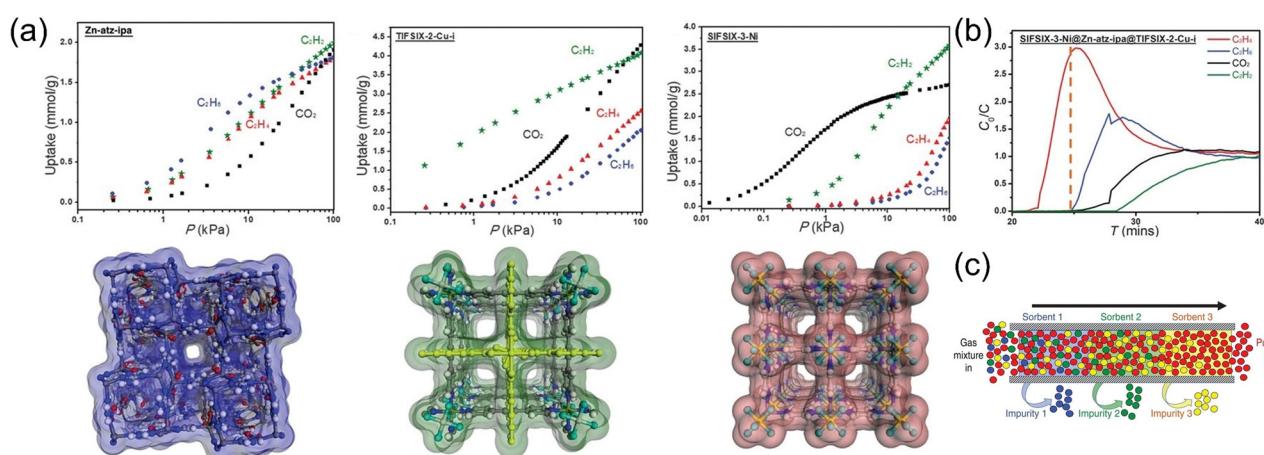
Fig. 9 (a) Structure and adsorption isotherms of three high-performance ultra-porous MOFs. (b) One step separation of high purity C_2H_4 in a four-component hybrid system. (c) Diagram of the synergy of the three MOFs. Reproduced with permission from ref. 4. Copyright © 2019, The American Association for the Advancement of Science.

means of molecular simulation, thereby analyzing the reasons for the selective adsorption of different gases by the three adsorbents in detail. SIFSIX series are a class of anion-functionalized MOFs, and the anions (SiF_6^{2-}, $NbOF_5^{2-}$, TiF_6^{2-}, AlF_5^{2-}) in the framework can be significantly different from the interaction between the guest molecules, thereby separating the mixed components.[69–71] Among them, SIFSIX-3-Ni has the highest adsorption selectivity because of its special structural characteristics, which can achieve strong tetradentate chelation for CO_2 molecules; TIFSIX-2-Cu-i can achieve strong linear double hydrogen bond binding to C_2H_2 molecules, so it has the strongest adsorption force for C_2H_2. Due to its unique pore structure, Zn-atz-ipa can form multiple weak hydrogen bonds with C_2H_6 molecules containing the most hydrogen atoms, thus having the highest adsorption selectivity for C_2H_6 molecules. Combining the advantages of the three, the one-step separation and preparation of C_2H_4 is finally realized. Additionally, the low-energy regeneration performance of the series adsorption column was also studied, and it was proved that the regeneration of the material could be completed after activation at 60 °C for one hour. This tandem adsorption column packing method is equivalent to arranging three adsorption columns in series, which is anticipated to greatly diminish the separation device size and simplify the sample activation procedure in future industrial applications. It supplies an advanced design idea for the research and development of green and low energy consumption processes under complex industrial separation systems.

In addition to the possibility of separating C_2H_4 from CO_2, C_2H_2, C_2H_4, and C_2H_6 mixtures in one step, the efficient preparation of C_2H_4 with multiple components through a single adsorption material still has more obvious technological advantages, such as simple packing process, uniform mass transfer process, easy sample molding, and high feasibility of scale-up experiments. Even so, the design and development of high-performance selective adsorption materials is relatively lacking. Through the precise structural design of MOF materials, Chen et al.[72] simultaneously embedded specific adsorption sites for a variety of impurity gases into a single porous adsorption material (Zn-atz-oba). The selective separation of C_2H_4 molecules from CO_2, C_2H_2, C_2H_4, and C_2H_6 in a single MOF was achieved for the first time, and then the high-purity preparation of polymer-grade C_2H_4 in a quaternary mixed system could be realized by only one-step adsorptive separation. Their work provides an important theoretical basis and candidate materials for the design of future C_2H_4 separation materials and the development of related multi-component chemical separation processes.

From the above examples, we can observe that whether NPU-1/2/3, UiO-67/67-$(NH_2)_2$, UPC-612/613 is used to separate C_2H_2/C_2H_4/C_2H_6, or MFSIX-17-Ni is used to separate C_2H_2/C_2H_4/CO_2, or TIFSIX-2-Cu-i/Zn-atz-ipa/SIFSIX-3-Ni is used to separate C_2H_2/C_2H_4/C_2H_6/CO_2, reticular chemistry is critical for the design and synthesis of these structures. The precise control of the molecular-level achieved by the reticular strategy is vital for fine-tuning the structure of MOFs for desired applications

and will be an essential approach for the design of materials with better C2 separation performance.

3.2 Separation of C3 mixtures

C_3H_6 is the second largest hydrocarbon product in the world after C_2H_4. By 2019, the global production capacity of C_3H_6 was as high as 129.8 million tons and is expected to reach 198.4 million tons by 2030,[73] but in the process of cracking to produce C_3H_6, impurities such as propyne and propadiene that are toxic to C_3H_6 polymerization catalysts are inevitably generated.[74] Therefore, the removal of trace amounts of C_3H_4 (less than 1%) and propadiene (about 5000 ppm) from C_3H_6 is of great industrial significance to generate high-purity C_3H_6 with impurities limited to less than 5 ppm or even less than 1 ppm. However, they have similar physicochemical properties, making the separation very difficult.[75–78] Currently, the traditional methods of catalytic partial hydrogenation or cryogenic distillation to convert or remove propyne and propadiene to acceptable levels are both energy consuming and inefficient.

The accurate size regulation and pore surfaces functionalization of MOF materials make them promising for petroleum-based platform compounds separation and purification. Through open metal sites, pore size regulation, and surface functionalization, the petroleum-based platform compounds' separation effect of MOFs can be improved, showing potential advantages in the purification of C_3H_6.[79–82] Bao et al.[83] reported a Ca-MOF with the capability of preferably trapping trace amounts of propyne and propadiene at low pressure. The material is fabricated from the low-cost precursor $CaCO_3$ and rigid squaraine. The adsorption isotherm shows that this Ca-MOF has record-breaking propyne (2.50 mmol g^{-1}) and propadiene (2.68 mmol g^{-1}) adsorption capability but exceptionally low C_3H_6 adsorption capacity (only 0.39 mmol g^{-1}) at 298 K and 5 mbar. When the pressure reached 1.0 bar, the selectivities for C_3H_4/C_3H_6 and propadiene/C_3H_6 with a volume ration of 0.5 : 99.5 were 38 and 54, respectively. Furthermore, in situ single crystal X-ray diffraction (SCXRD) analysis and DFT simulations obviously demonstrated the strong host–guest hydrogen bonds and $\pi \cdots \pi$ interactions.

The one-step separation of multi-component petroleum-based platform compounds using a single adsorbent can greatly elevate the separation efficiency, though it is also a great challenge due to the difficulty of accurately preparing MOF materials with multiple gas-binding sites. Xing et al.[84] prepared an interspersed MOF structure, ZU-62 with $NbOF_5^{2-}$, as the anion column (Fig. 10). Compared with their previously reported anion column SiF_6^{2-} of SIFSIX-2-Cu-i, $NbOF_5^{2-}$ possesses an asymmetric O/F coordination site, which can simultaneously capture propyne and isoprene in C3 mixtures. The unique coordination geometries within ZU-62 form different nanospaces (6.75, 6.94, and 7.20 Å for site I, site II, and site III, respectively) provide corresponding binding sites for propadiene and propyne, enabling the simultaneous adsorption of propyne (1.87 mmol g^{-1}) and propadiene (1.74 mmol g^{-1}) at 5000 ppm. The trapping mechanism was revealed by DFT and GCMC calculations. In addition, they synthesized two anionic
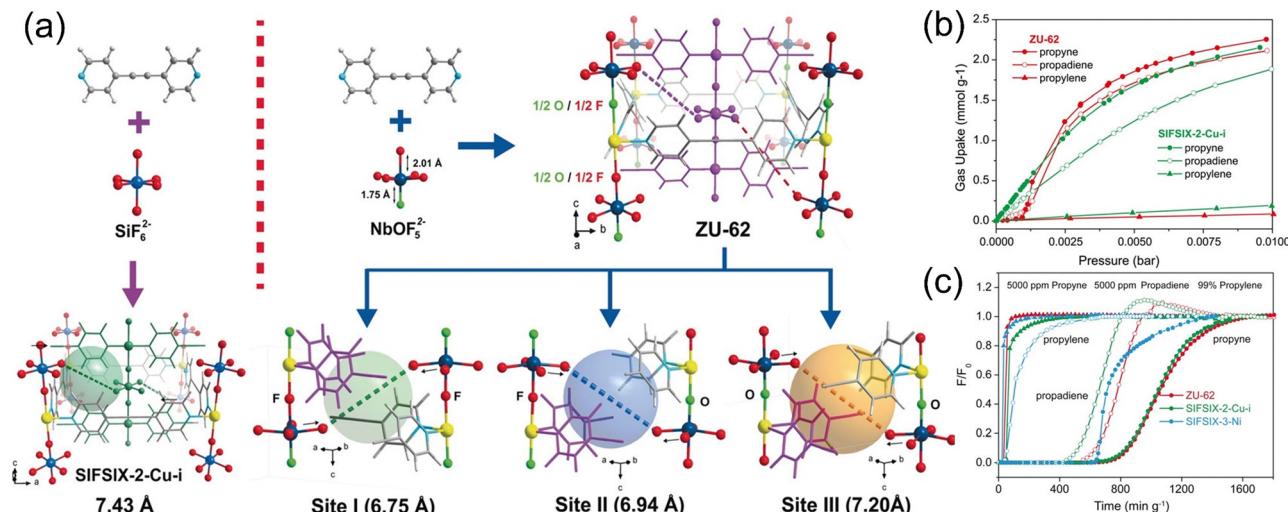
Fig. 10 (a) Structure and (b) propyne/propadiene/propylene adsorption isotherms of ZU-62 and SIFSIX-2-Cu-i. (c) The experimental column break-through curves for propyne/propadiene/propylene (0.5 : 0.5 : 99, v/v/v) separation. Reproduced with permission from ref. 81. Copyright © 2018, Wiley-VCH Verlag GmbH & Co. KGaA, Weinheim.

pillared hybrid ultra-microporous MOFs (ZU-16-Co[85] and ZU-33[86]). The simultaneous adsorption and disposal of trace amounts of C_2H_2 and C_3H_4 from $C_2H_2/C_2H_4/C_3H_4/C_3H_6$ and $H_2/CH_4/C_2H_2/C_2H_4/C_2H_6/C_3H_4/C_3H_4(PD)/C_3H_6/C_4H_6/n$-$C_4H_8/i$-$C_4H_8$ mixture was achieved by introducing different binding sites and fine-tuning the aperture to match the shape of petroleum-based platform compounds.

In addition, Ji et al.[87] reported an ultra-microporous Zn-MOF capable of trapping trace amounts of C_3H_6 and efficiently separating $CH_4/C_2H_4/C_2H_6/C_3H_6/C_3H_8$ (3/5/6/42/44, v/v/v/v/v). This Zn-MOF exhibited exceptional ability to capture propylene at lower pressures, boasting a new record for C_3H_6 uptake at 298 K (34.0/92.4 cm^3 cm^{-3} at 0.01/0.1 bar). This was due to multiple binding interactions and swift diffusion behavior, resulting in a quasi-orthogonal configuration of C_3H_6 in adaptive channels. Furthermore, the scale-up of low-cost activated Zn-MOF to separate equimolar C_3H_6/C_3H_8 mixtures could produce 30.8 L of propylene with a purity of 95.0–99.4%.

In conclusion, "tailoring" is an effective means to design porous adsorbents. According to the shape characteristics of C3 molecules, three strategies are applicable: (1) constructing suitable micropore channels in the framework of MOFs, with the aid of comprehensive pore regulation to construct multiple cooperative functional sites and enhance the "specificity" and "affinity" of C3 molecules; (2) the construction of single molecular traps is an effective method to selectively capture trace gases from C3 multi-component mixtures with similar molecular structures; (3) for conventional adsorbents that cannot achieve the multi-component separation of C3 by the size sieving mechanism, the construction of flexible-rigid MOFs not only has the unique molecular recognition effect of flexible MOFs but also takes into account the higher adsorption capacity of rigid MOFs at low pressure. Thereby, the one-step

high-efficiency separation of C3 multi-components can be achieved.

3.3 Separation of C4 olefins

1,3-Butadiene is one of the most important chemical basic raw materials that finds extensive application in the manufacturing of synthetic rubber. It is usually separated from other C4 hydrocarbon mixtures such as butane, butene, and isobutene through a relatively energy-intensive extractive fractional process.[88–90] It is currently difficult to preferentially isolate 1,3-butadiene using porous materials because most porous materials selectively adsorb olefins with higher polarity, smaller volume, and stronger coordination ability. In contrast, MOFs have many advantages in the adsorption and separation of C4 hydrocarbon, such as the separation with kinetics, enthalpy interactions, pores, and guest responses, by introducing open metal sites and functionalized hydrophobic surfaces to improve their C4 hydrocarbon separation performance. However, the separation effect of a single separation mechanism is limited. If a more precise separation mechanism can be used, the separation performance of specific MOF materials for C4 hydrocarbon can be better improved.

In order to solve this problem, Zhang et al.[91] proposed the concept of "controlling the configuration of flexible guest molecules to reverse the adsorption selectivity", that is, by changing parameters such as the aperture and shape of MOFs. By controlling the conformation of the adsorbed guest molecules, the difference in the flexibility of the guest molecules can be used to significantly reduce the adsorption enthalpy of 1,3-butadiene relative to other C4 hydrocarbon molecules, which can realize the reversed adsorption selectivity. For porous frameworks, large pore sizes are not conducive to controlling the conformation of guest molecules, while small pore sizes can only accommodate guest molecules with elongated shapes in

the *trans* conformation. Combined with factors such as guest diffusion, flexible MOFs with independent cavity structures and continuous pore channels may become ideal adsorbents. They carried out proof-of-concept for 10 MOFs with three types of representative structures by means of mixed gas adsorption breakthrough experiments, single-component gas adsorption experiments, single crystal diffraction experiments, and computer simulations. The results of the study show that the MAF-23[92] they designed and synthesized earlier can achieve an abnormal and optimal C4 hydrocarbon adsorption and separation sequence. MAF-23, with its quasi-discrete cavity structure, induces a conformational change of the flexible guest molecule, which can be weakened by the MOF adsorption through the bending of the 1,3-butadiene guest molecule. Under 298 K and 1 bar, when the C4 hydrocarbon mixture flows through the adsorption device with MAF-23 as the filler, 1,3-butadiene molecules flow out first, followed by butane, butene, and isobutene. Therefore, using MAF-23 as the main adsorption material can achieve the weakest adsorption and efficient purification ($\geq 99.5\%$) of 1,3-butadiene at mild conditions and avoid possible polymerization in high temperature environments.

The precise control of pore size and shape is critical for the C4 multi-component separation performance of ultra-microporous and flexible materials. Xing *et al.*[93] reported a class of hybrid ultra-microporous materials with interpenetrating structure. By changing the anion columns, the aperture can be varied within a small range. The material has flexible pores for molecular recognition and size screening and has a large-capacity screening effect for C_4H_6/iso-C_4H_8, C_4H_6/n-C_4H_8,

indicating that the combination of size sieving effects and targeted molecular recognition is a powerful strategy for separating olefin isomers. It discriminates multiple differences in the molecular shape/size and characteristics of C4 olefins to maximize separation efficiency. They also reported the sulfonate anion-pillared hybrid ultra-microporous materials (TMOF-1 and ZU-619) that can efficiently separate ternary C4 olefin mixtures (C_4H_6/n-C_4H_8/iso-C_4H_8), which marks the first successful application of such materials.[88] The interpenetrating direction of the sulfonate anions is tuned by changing the length of the anions, thus judiciously controlling the geometry of the adsorption sites. In addition, Bao *et al.*[94] reported a series of gallic acid-based MOFs (M-gallate, M = Ni, Mg, Co) whose elliptical pore is well suited for the shape-selective separation of *trans/cis*-2-butene through the differentiation of *trans/cis*-2-butene on the smallest molecular cross-sectional size (Fig. 11). M-Gallate not only has the maximum *trans/cis*-2-butene selectivity but also achieves the high-efficiency separation of 1,3-butadiene, 1-butene, and isobutene. DFT calculations suggest that Mg-gallate interacts strongly with 1,3-butadiene and *trans*-2-butene, and the C···H–O synergistic supramolecular interaction distances are 2.45–2.79 and 2.57–2.83 Å, respectively. In the breakthrough experiment, Mg-gallate not only showed excellent *trans/cis*-2-butene separation capability but also achieved the separation of 1-butene/isobutene binary mixtures and 1,3-butadiene/1-butene/isobutene ternary mixtures. Kitagawa *et al.*[95] designed and synthesized a MOF $[Zn(NO_2ip)(dpe)]_n$ (SD-65) with flexible structure and suitable cavity size, providing accommodation for specific guest molecules. The material can adsorb 1,3-butadiene from six
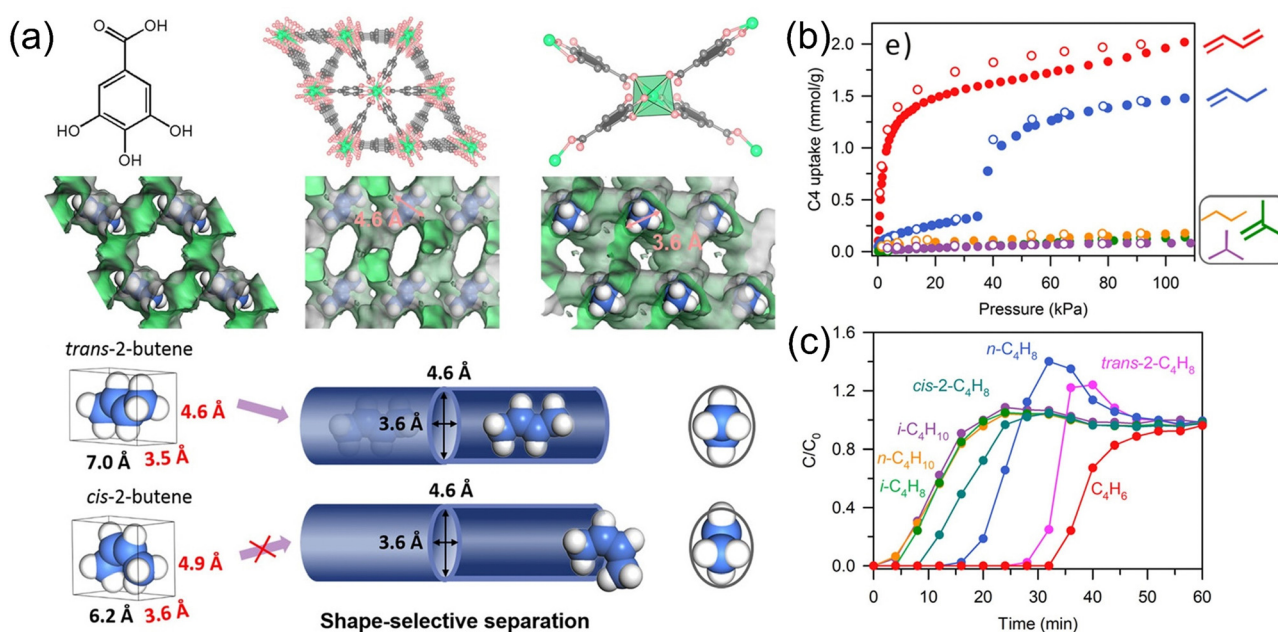
Fig. 11 (a) Structure, channel, and separation of *trans*-and *cis*-2-butene of M-gallate. (b) Adsorption isotherms of *trans*-2-butene, *cis*-2-butene, 1,3-butadiene, 1-butene, iso-butene, n-butane, and iso-butane on Co-gallate at 298 K. (c) Mixture breakthrough curves on Mg-gallate for 1,3-butadiene/1-butene/iso-butene/n-butane/iso-butane/*trans*/*cis*-2-butene/He (20/10/10/5/1/2/2/50) at 298 K. Reproduced with permission from ref. 91. Copyright © 2020, American Chemical Society.

isomers of C4 (*n*-butane, 1-butene, *trans*-2-butene, *cis*-2-butene, isobutene, and 1,3-butadiene). The separation performance of SD-65 was demonstrated by adsorption isotherms, solid-state NMR, *in situ* XRD, multi-component gas adsorption, and gas adsorption–desorption cycling experiments.

Based on the diversity of the C4 molecular structure, on the one hand, the rigid framework structure can be used to control the configuration change of the C4 molecule, and on the other hand, the flexible structure can be designed to adapt to the C4 molecule, and C4 molecule specific recognition can be achieved using the molecular sieving effect or enhancing the host–guest interaction.

4 Separation of liquid or vapor from petroleum-based platform compounds

MOFs have a wide application in C1–C4 hydrocarbons separation, and the understanding of their adsorption and separation mechanisms has been relatively mature. The rational design of MOFs can be basically achieved by regulating the host–guest van der Waals forces, introducing open metal sites, hydrogen bonding and other weak interactions, which can achieve the desired effects for specific mixture systems. However, since the phase forms of C6 and C8 are different from C1–C4 gases, the adsorption and separation of MOFs in liquid/vapor phase C6 and C8 compounds is still in the exploratory stage. In addition, the mechanism of host–guest interaction has not been fully revealed and the unique pore chemical environment of MOFs is ignored; thus, the rational design of specific MOFs for separation of isomers has not been fully realized.[96]

It is relevant to separate hydrocarbon molecules, such as Bz/Cy and *OX/MX/PX*, for their broad application as chemical raw materials but also challenging due to their similar molecular sizes and close boiling points. Physical separation could provide an energy-efficient settlement to this problem, but designing and combining sorbents with high selectivity for one of these hydrocarbons is still a significant obstacle.

4.1 Separation of C5 olefins

C5 olefin is a kind of valuable chemical raw material, which is composed of active olefin and diolefin. Among them, isoprene accounts for 15% to 25% of the C5 portion, which is commonly used in the manufacture of medicine, synthetic rubber, and pesticide intermediates. 1-Pentene and *trans*-2-pentene are significant as alpha- and beta-olefins. At present, the pure components are mainly obtained *via* solvent extraction distillation technology in industry. However, this process is energy-intensive and environmentally unfriendly. In addition, highly reactive double bonds present in olefins often lead to polymerization at elevated temperatures during the distillation process, resulting in low separation efficiency. Another potential energy-saving strategy is adsorptive separation technology. However, when it comes to the separation of olefin isomers, which have molecular shapes and lengths that are nearly identical except for the position of the double bond; thus, finding appropriate separation materials poses a significant challenge.

In view of this, Cui *et al.*[97] reported two MOFs (TIFSIX-2-Cu-i and ZU-62) for C5 olefin separation (1-pentene, *trans*-2-pentene, and isoprene). At 298 K and 45 kPa, TIFSIX-2-Cu-i can distinguish *trans*-2-pentene from three C5 olefins with high adsorption (3.1 mmol g^{-1}) based on the electrostatic environment distribution of TiF$_6^{2-}$, and adaptive structural changes enhance the recognition of 1-pentene and *trans*-2-pentene (Fig. 12). ZU-62 with smaller aperture exhibits molecular sieving effect on isoprene in the low pressure (0–6 kPa) range, with a high 1-pentene/isoprene selectivity of 300. Breakthrough experiments further demonstrated the 1-pentene/isoprene separation
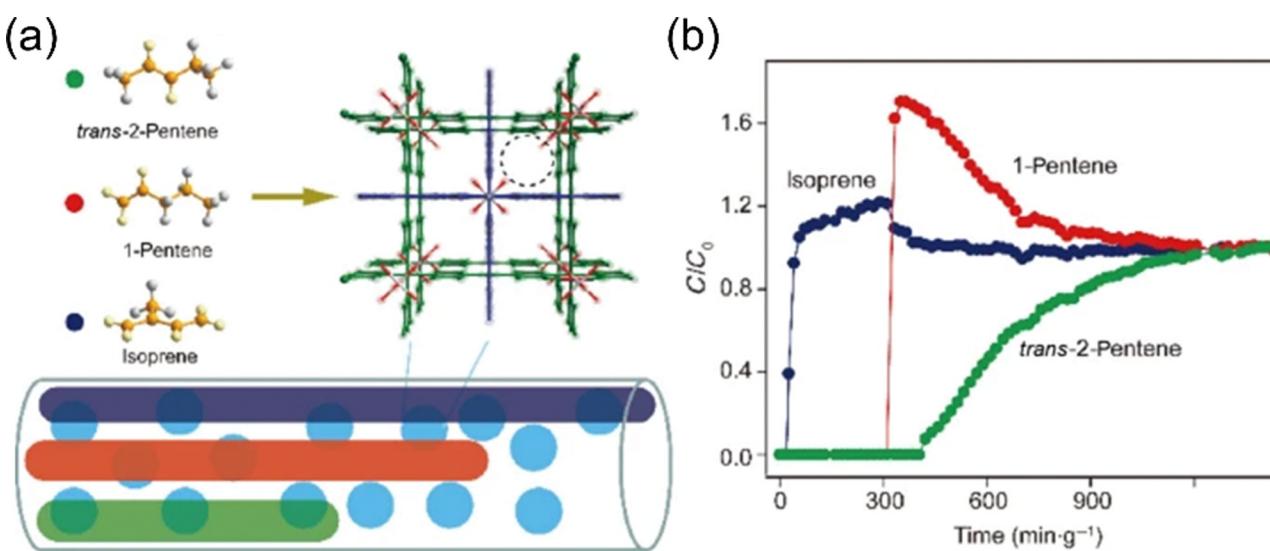

Fig. 12 (a) Schematic diagram of TIFSIX-2-Cu-i and ZU-62 for the separation of *trans*-2-pentene/1-pentene/isoprene. (b) The breakthrough performance of TIFSIX-2-Cu-i for *trans*-2-pentene/1-pentene/isoprene/N$_2$ (9%/9%/9%/73%, v/v/v/v) ternary mixtures. Reproduced with permission from ref. 94. Copyright © 2021, Springer Nature Publishing AG.

performance of ZU-62. Meanwhile, the simulation study further revealed the special adsorption behavior inside the pores.

Drawing on the design strategy of C2–C4 multi-component separation materials, the rapid development of crystal engineering and reticular chemistry will provide guidance for C5 multi-component separation.

4.2 Separation of C6 isomers

In the petrochemical industry, the separation of HEX isomers is classified based on the degree of branching, such as the separation of di-branched 22DMB and 23DMB from mono-branched 2MP and 3MP and linear n-HEX, which is essential to produce high-octane gasoline. Currently, catalytic isomerization is utilized to transform straight-chain alkanes to their branched-chain isomers; however, the isomer mixture produced by this process requires work-up to obtain the di-branched-chain hexane isomers with the highest-octane numbers. But their similar physicochemical properties make the separation of these isomers very challenging. Adsorptive separation based on porous material greatly reduces energy consumption and CO_2 emissions compared to current large-scale distillation processes for separating C6 alkane isomers. As the benchmark adsorbent, 5A zeolite, due to its suitable pore size, can adsorb linear alkanes, excluding di- and mono-branched isomers. Furthermore, it can be used as a supplement to distillation in the industry. However, its adsorption capacity is relatively low, which constrains its separation efficacy. As such, it is urgent to find alternative adsorbent materials.

Compared with traditional zeolite materials, MOF materials can easily fine-turn the pore size by adjusting organic ligands and secondary building units. The kinetic diameters of n-HEX, 3MP, and 22DMB are 4.3, 5.0, and 6.2 Å, respectively. To achieve the separation of the three liquids, MOF materials with suitable size should be designed. Chen et al.[98] synthesized MOF-1 for hexane isomers separation. Along the a-axis direction of MOF-1 is a 7.5 × 7.5 Å^2 channel, and 3.8 × 4.7 Å^2 channels along the b- and c-axis directions are viewed. The a-axis direction can allow three molecules to pass through, but the larger kinetic diameter of n-hexane endows it with a larger van der Waals force with the pore wall. The b-axis and c-axis pores allow n-hexane to pass through and block 3MP and 22DMB. The dynamic separation of hexane isomers by microporous MOFs can be achieved with this simple fixed-bed adsorption method. Furthermore, Long et al.[99] presented a highly stable $Fe_2(bpd)_3$ with triangular channels that can classify hexane isomers depending on the degree of branching separation (Fig. 13). The adsorption isotherms and adsorption heats indicated that the order of adsorption selectivity was n-HEX > 2-ethylpentane > 3MP > 23DMB ≈ 22DMB. The di-branched isomer elutes first from a bed filled with $Fe_2(bdp)_3$, then the mono-branched isomer, and finally is linear n-HEX, during the breakthrough experiment for the equimolar mixture at 160 °C.

For the separation of single and double branches of C6 alkanes, Li et al. have done a lot of meaningful work. First, they[100] developed a highly stable Al-MOF with two one-dimensional channels (Al-bttotb/467-MOF) and used rigid MOFs for the first time for the complete sieving of single- and double-branched isomers of C6 alkanes. The average pore size of the channel (5.6 Å) is between those of single-branched (3MP: 5.5 Å) and double-branched (22DMB: 6.2 Å) C6 alkanes, enabling the efficient adsorption of n-HEX (linear) and 3MP (151 and 94 mg g^{-1}, 30 °C) but did not adsorb their double-branched isomers at all. The separation effect is much higher than the reference material 5A zeolite. Gas separation experiments illustrate that Al-bttotb can separate n-HEX, 3MP, and 22DMB mixtures. At the same time, for the mixture of five components (n-HEX, 2MP, 3MP, 23DMB, and 22DMB), it also has the effect of separating double branched paraffins from other isomers. SCXRD and adsorption simulations further demonstrate that n-HEX or 3MP is adsorbed in smaller square channels in pairs, and the appropriate channel size enables Al-bttotb to exhibit selective adsorption behavior among C6 alkane isomers. In addition, they[101] also reported a Ca-MOF, $Ca(H_2tcpb)$, which also achieved the complete separation of linear, single-branched, and double-branched alkane isomers. This separation technology, which can completely screen paraffin isomers with single and double-branches, can not only obtain gasoline with higher octane number but also fill the gap in current separation technology. Through het XRD analysis of different adsorption forms, they attributed the unique adsorption and separation performance of the material to its structural characteristics and different forces on different alkane isomer molecules. The crystal structure of the material has a certain flexibility, and it has a specific effect on the adsorption of different alkane isomer molecules. The adsorption effect on the same molecule at different temperatures is also different; thus, it can achieve effective separation under temperature control. Further, they[102] reported a series of stable Zr-MOFs with optimized pore structures through topology-directed design and synthesis for the efficient separation of C6 alkane isomers. The selective recognition of C6 alkane isomers can be achieved by rationally designing MOFs with different rigidity or flexibility through the rational selection of organic linkers, which provides the petroleum refining industry with a complementary, straightforward technology to further increase the octane rating of commercial gasoline products.

In addition to designing and synthesizing novel MOF materials, more interestingly, Ghoufi et al.[103] proposed to tune the aperture/shape of ZIF-8 upon adsorption by applying external mechanical pressure. The adsorption performance of ZIF-8 for C6 isomer single-component and binary mixtures under mechanical pressure was predicted by molecular simulations integrating molecular dynamics (MD) and GCMC technique and incorporating a Hybrid Osmotic Monte Carlo (HOMC) scheme. Compared with pristine ZIF-8, the selectivity of n-HEX/2MP and 2MP/2,3-dimethylbutaneby for modified ZIF-8 is expected to increase by 40% and 17%, respectively, under mechanical pressure above 1 GPa.

The separation of C6 and C8 isomers was performed under conditions corresponding to pore saturation.[104,105] Such separations are governed by entropy effects and packing
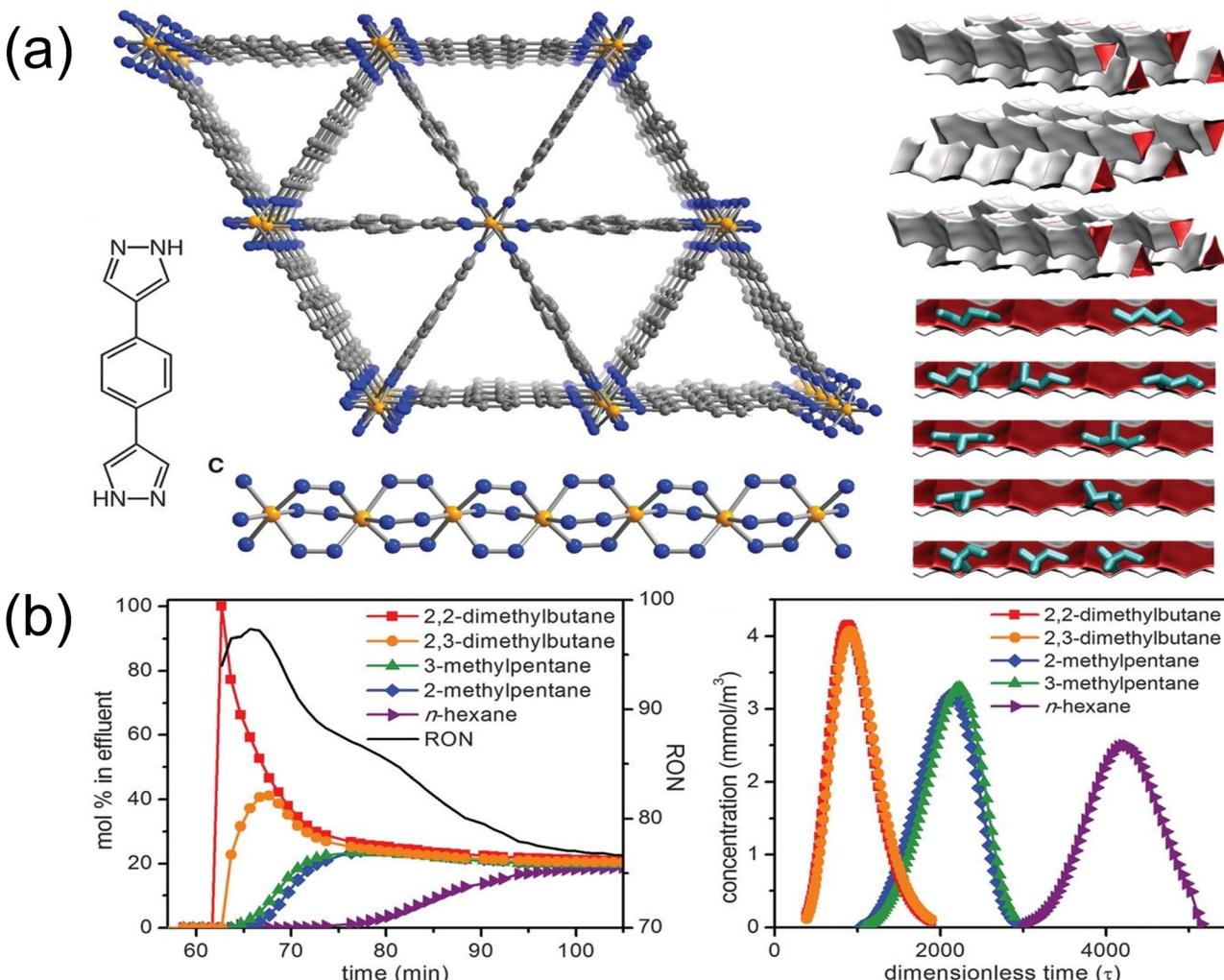
Fig. 13 (a) Structures of $Fe_2(bdp)_3$. (b) Mixture breakthrough curves of an equimolar mixture of 2,2-dimethylbutane, 2,3-dimethylbutane, 3-methylpentane, 2-methylpentane, and *n*-hexane running through a packed bed of $Fe_2(bdp)_3$ at 160 °C. Reproduced with permission from ref. 96. Copyright © 2013, The American Association for the Advancement of Science.

efficiencies. Kinetic diameters are irrelevant. The separation of C6 isomers highly depends on the geometric shape and size of the microporous channels. For example, the optimal stacking of OX parallel to the diamond channel walls of 8.5 Å in MIL-47 and MIL-53 leads to strong selectivity towards OX. The difference in the stacking efficiency of linear and branched C6 isomers is commonly referred to as the configurational entropy effect, which can be effectively used to separate C6 isomers and obtain various products with different branching degrees.[101] Taking MFI zeolites as an instance, linear isomers can be comfortably located along both straight and Z-shaped channels. On the contrary, mono-branched and di-branched isomers with steric hindrance prioritize to locate at the channel intersections that provide more space for branching. Due to the limitation of 4 crossover sites per unit cell, the saturation capacity of the di-branched isomers is limited to 4 molecules per unit cell. When operating under conditions close to saturation, the difference in packing efficiency leads to sharp separation. Recognizing the importance of entropy effect enables us to

select or develop materials or channel topologies that contribute to the effective packing of selectively adsorbed components. Dubbeldam *et al.*[106] found that the enthalpies for mono-branched molecules are higher than *n*-HEX, and the enthalpies of di-branches are even higher in energy.

Adsorption-based separation depends on the adsorption or diffusion properties. At low loadings (*i.e.*, the Henry regime), the selectivity is predominantly determined by enthalpic effects and favors the molecule exhibiting the strongest interaction with the framework. Selectivity is hence closely linked to the properties of both the adsorbent and the adsorbate, including dipole moment, polarizability, quadrupole moment, and magnetic susceptibility. Under saturation conditions (industrial setup), the selectivity is driven by either enthalpic effects and/or entropic effects, including various phenomena such as "commensurate freezing",[107] which accentuates molecules whose size correlates with the dimensions of the channel; "size entropy",[108,109] which favors the smallest molecules; "length entropy",[108,110–112] which favors the molecules with the

shortest effective length (footprint) in one-dimensional (1D) channels; "commensurate stacking",[113] which favors molecules with stacking arrangements that are commensurate with the dimensions of one-dimensional channels; and "face-to-face stacking",[114] which facilitates molecules that upon reorientation reduce their footprint significantly in one-dimensional channels. Such selectivity factors play significant roles in determining which molecules are favored in specific channels within a given system.

Enthalpy mechanisms have the potential to increase selectivity in molecular separations, but their application is primarily limited to low loading ranges. As a result, these mechanisms cannot take advantage of all the large pore volume that MOFs could provide. Industrial processes typically operate at pore saturation. Therefore, one should focus on entropic molecular segregation mechanisms that can operate under such conditions. Recent approaches have shown that high selectivities can be achieved at high pore loadings, and therefore, such methods deserve attention.[115]

A careful comparison of the performance of various MOFs and zeolites leads to the conclusion that the MFI zeolite is perhaps the most promising adsorbent.[59,116–118] For MOFs, multiple non-covalent interactions between guest molecules and framework can be generated by regulating the pore size and pore environment, which is the key to achieve the selective adsorption of C6 isomers and has the advantages of high adsorption capacity and long breakthrough time.

4.3 Separation of C8 aromatics

Xylene aromatic mixtures are used as antiknock additives and synthetic chemical solvents in gasoline, and each pure isomer also has its own purpose. PX is a precursor of polyethylene terephthalate and polybutylene terephthalate, MX can be applied to produce isophthalic acid, and OX can be transferred into phthalic anhydride, which is an intermediate in coatings and plasticizers. Currently, all three isomers can be separated by crystallization along azeotropic or extractive distillation, but the process is complex and energy-intensive. Based on the kinetic diameter, the smaller PX (0.58 nm) can be separated from OX (0.65 nm) and MX (0.64 nm) by molecular sieves.[119] Nevertheless, the separation of MX/OX is still a very tough task. Consequently, finding a feasible method to replace the traditional separation process has been the key to the modern chemical industry.

Adsorptive separation is an efficient and energy-saving technology that has been widely applied in hydrocarbon isomers separation. At present, the simulated moving bed technology is mainly used in the industry, and the traditional faujasite X-type and Y-type molecular sieves are used as adsorbents. The Y-type molecular sieve exchanged with K^+ or Ba^{2+} can selectively adsorb PX with subtle entropy effects to realize the separation of xylene isomers, but its adsorption capacity is low.[59,104,113] In terms of adsorbent modification, the adsorption capacity of ADS-37 launched by UOP in 2004 is 6% higher than that of the previous generation ADS-27. Subsequently, ADS-47, which was launched in 2011, has achieved certain improvements in

adsorption capability and mass transfer performance. The adsorption capacity of the second-generation adsorbent RAX-3000A launched by Sinopec is 8% higher than that of the first-generation RAX-2000A, and it was first applied to the SorPX-simulated moving bed adsorptive separation process developed by Sinopec in 2011.

The above adsorbents are all based on faujasite molecular sieve materials. After more than ten years of continuous improvement, their adsorption performance is close to the limit. Therefore, how to design and screen new materials to break through the limitations of traditional faujasite materials is of great significance. Since MOF acts as a physical adsorbent, its pore size can be adjusted and the pores can be functionalized, which solves the problem of separation selectivity.[120–122] Cui et al.[123] designed and prepared a guest-responsive anionic pillared framework material (ZU-61), whose topology is different from that of traditional faujasite material molecular sieves (Fig. 14). The adsorption capacity for MX is 3.4 mmol g^{-1}, which is superior to that of NaY (1.7 mmol g^{-1}). Most importantly, the $NbOF_5^{2-}$ anion site in the framework has rotational flexibility, which can rotate to different degrees according to different xylene isomer guest molecules and identify the slight differences between the isomers. The three-component gas phase breakthrough experiment also verified the excellent separation performance and cycle stability of ZU-61 for xylene isomers. Adsorbents are always the key factor to the advancement of adsorptive separation technology, and this work provides important ideas for exploring new separation materials and new separation mechanisms.

Furthermore, Sapianik et al.[124] reported a novel heterometallic MOF (NIIC-30(Ph)) with a special tortuous pore with aromatic adsorption sites, exhibiting record high selectivity for PX/OX (3.03). Simultaneously, at least three separation cycles can be achieved for the ternary OX/MX/PX mixture in liquid and gas phase. Gaining insight into the adsorption behavior of NIIC-30(Ph) by studying the structure of aromatic guest in MOF, there are two most important factors affecting the preferential adsorption of OX to PX and MX. First, compared to the other two isomers, the OX is stabilized by less $C–H\cdots\pi$ and $CH_3\cdots\pi$ interactions in the structure. The second is that the rigid framework does not wish to deform to accommodate guest molecules, which is optimal in the OX structure. Long et al.[122] reported a class of MOFs Co_2(dobdc) and Co_2(m-dobdc), and the PX isomers separation performance was tested by single-component adsorption isotherm and multi-component breakthrough experiments. It is worth noting that Co_2(dobdc) can discriminate all four molecules, and the binding affinity follows the order OX > EB > MX > PX. Multi-component liquid phase adsorption experiments further confirm the selectivity in a wide concentration range. Both frameworks facilitate separation by the degree of interaction between the two adjacent Co^{2+} centers and C8 guest molecule, and the capability of each isomer to fill within the framework, according to the structural characterization of SCXRD. Furthermore, Co_2(dobdc) distorts its structure when combined with OX or EB, which considerably enhances its adsorption capacity.
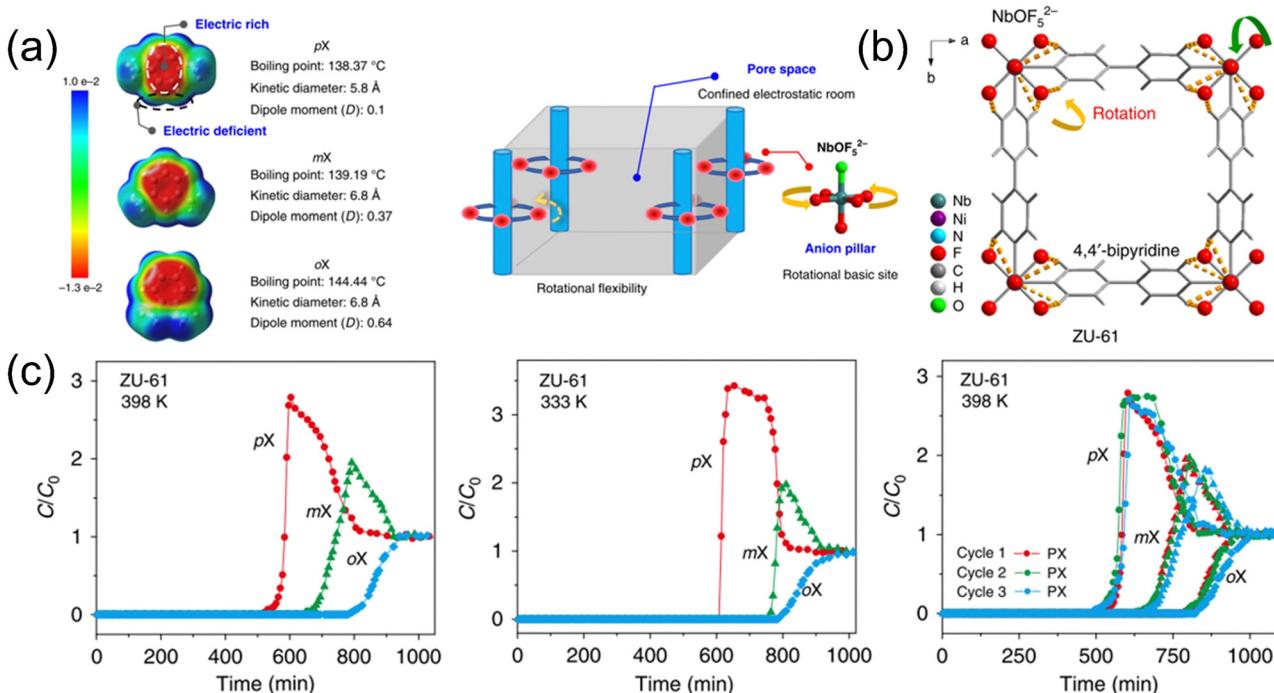
Fig. 14 (a) Electron density (e a.u.$^{-3}$) of each xylene isomer and schematic illustration of the porous adsorbent with Lewis basic–binding sites and rotational flexibility. (b) Structure of ZU-61 with the rotational ligand of the NbOF$_5^{2-}$ anion and bipyridine. (c) Breakthrough curves for PX/MX/OX (1:1:1) separations with ZU-61. Reproduced with permission from ref. 120. Copyright © 2020, Springer Nature Publishing AG.

Recently, Farha *et al.* obtained two cases of MOFs (NU-2000 and NU-2001) that are isoreticular to MIL-53 through pore engineering. Using the difference in the pore size in the framework, xylene isomers can be effectively separated under ambient conditions.[125] At 5 mbar, the adsorption capacities of NU-2000 and NU-2001 for PX were 2.1 and 1.9 mmol g^{-1}, respectively, with calculated selectivity values of 20 for PX/OX and 3.9 for PX/MX. Bao *et al.* developed a stacked 1D coordination polymer [Mn(dhbq)(H$_2$O)$_2$] with 1D chains of hydrogen bonds, multiple open metal sites, abundant π-electrons, as well as a high level of structural flexibility.[126] Its unique temperature-dependent adsorption behavior enables the complete separation of OX, MX, and PX isomers in both gas and liquid phases. The fine stimulation-responsive expansion of the structure endows this porous material with extreme flexibility and stability, well-balanced adsorption capacity, high selectivity, and fast kinetics that are particularly suitable for industrial conditions. These studies provide an alternative approach for energy-efficient and adsorption-based xylene separation and purification processes in industry.

A further point to note is that the feed mixtures contain OX, MX, PX, and EB. Industrially, the demand for PX is the highest amongst the xylenes, and PX-selective MOFs are required as potential replacements for traditional adsorbents. Although the discussion is all about OX selectivity, the preferential extraction of PX is also beneficial.[127] For example, Ghosh *et al.*[128] reported the framework flexibility-driven selective sorption of PX over other isomers by DynaMOF-100. Zaworotko *et al.*[129] reported another benchmark C8 adsorbent, sql-1-Co-NCS, with highly

selective and high-capacity separation of OX from C8 aromatics.

Styrene is an important monomer for synthetic rubbers, thermoplastics, and resins. The catalytic dehydrogenation of ethylbenzene is the main method to produce styrene, which is reversible and thermodynamically unfavorable, thus containing many reactants and by-products, such as benzene and toluene. Due to the similarities in the physical properties of these molecules as well as the high reactivity of styrene, complex processes are required to separate the mixture in the industry. For example, vacuum/extractive distillation uses about 80 trays and at least four distillation columns to produce high-purity styrene. Adsorptive separation using molecular sieve effect instead of distillation is a promising method. So far, only one case on the molecular sieve separation of styrene/ethylbenzene is reported because of the challenges in the precise design and control of pore size. Zhang *et al.*[130,131] reported a Cu(I)-MOF (MAF-41) with limited flexibility, exhibiting an intermediate size molecular sieve effect. Single-component isotherms exhibit adsorption of styrene but completely exclude larger ethylbenzene (size exceeds maximum pore size) and smaller toluene/benzene (adsorption energy is not enough to open the cavity). Breakthrough experiments showed the selectivity of styrene up to 1250 for equimolar ethylbenzene/styrene mixtures and 3300 for equimolar ethylbenzene/styrene/toluene/benzene mixtures. In a single adsorption–desorption cycle, more than 99.9% pure styrene can be produced. Furthermore, the separation of ethylbenzene/styrene mixtures using MOFs relies primarily on the fact that styrene is a planar molecule while ethylbenzene is
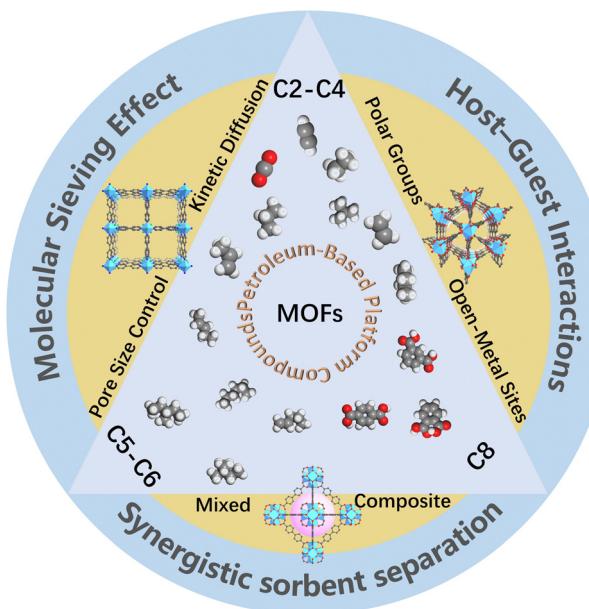
Fig. 15 Schematic diagram of metal–organic frameworks for the separation of petroleum-based compounds.

not.[59,104,113,132] The work of Torres-Knoop *et al.*[113,132] clearly shows that the separation of ethylbenzene/styrene mixtures with MOFs relies on the difference in the planarity of the two guests. In addition, there are also several reports of low dimensional materials for C8 separation, such as 0D materials[133,134] and 2D materials.[129]

Molecular sieving plays a vital role in the process of C8 separation. In addition to basic synthetic design strategies, machine learning-assisted computational screening of pore size-based shape-selective MOFs will be efficient and beneficial in accelerating the discovery of novel MOFs for the separation of C8 aromatic molecules, which will be a new trend to synthesize functionally-oriented MOFs.

5 Conclusion and outlook

The purification of petroleum-based platform compounds is a hot and important topic. Conventional separation techniques rely heavily on liquid adsorbents or cryogenic distillation, which are energy-intensive and costly. Contrarily, the novel non-thermally driven adsorptive separation technology has broader application expectations. The selection of an adsorbent is very important for adsorptive separation. Due to their permanent porosity, modular nature, and chemical customizability, MOFs show great potential for application in the separation of petroleum-based platform compounds. We briefly review novel adsorption separation techniques and their mechanisms, focusing on recent advances in MOFs for the separation of various multi-component petroleum-based platform compounds. In our opinion, the current design of MOF materials applied to the separation of multicomponent petroleum-based platform compounds mainly focuses on three aspects: (1)

realization of the molecular sieving effect through the precise regulation of pore size and pore shape; (2) selective enhancement of recognition adsorption of specific molecules achieved through post-functionalization or opening of metal sites; (3) realization of $1 + 1 > 2$ separation effect utilizing multiple MOF materials with different functions in the form of mixed or composite (Fig. 15).

In the future, to achieve the efficient separation of multi-component petroleum-based platform compounds with MOF adsorbents, the following issues need to be addressed from academia to final industrial implementation.

(1) In the process of promoting the large-scale application of MOF materials, the stability of MOFs will surely receive more attention. Although MOF materials are connected by strong interactions between organic–inorganic building blocks, their use in harsh environments still faces challenges. Therefore, compounding MOF with other protective functional materials or modifying MOF in a function-oriented manner to improve its stability may fundamentally solve this problem.

(2) The development of MOF adsorbents plays a crucial role in reducing energy for multi-component separation. To meet the needs of practical applications, it is imperative to enhance the equilibrium between target compound selectivity and adsorption capacity in the multi-component separation procedure. In terms of structural design, MOF synthesis has developed from exploration and trial-and-error to precise design. However, there is still a lack of guidance on the precise synthesis route of MOF structures. Therefore, in the application of adsorbents, the future development trend is to explore an energy-saving and ecologically friendly separation route of functionally-oriented MOFs through microstructure design optimization, striving to achieve the efficient separation of petroleum-based platform compounds.

(3) At present, adsorptive separation technology has made great progress, but it is still in the rising stage of development after all, and the existing adsorption and separation processes need to be further improved and perfected. To promote adsorptive separation technology from the laboratory to the factory, the actual chemical mixture and engineering conditions should be considered, the economics and sustainability of adsorptive separation technology (stability and cost of the adsorbent) should be evaluated, and the scale of adsorptive separation technology in practical application in the industry should also be considered. The continuous exploration and development of new processes and materials and the expansion of the original application fields will make adsorptive separation technology more important.

Abbreviations

dobdc	2,5-Dioxa-1,4-phthalate
mdobdc	4,6-Dioxo-1,3-phthalate
batz	(Bis(5-amino-1*H*-1,2,4-triazol3-yl)methane)
bpd	1,4-Benzenedipyrazolate
dhbq	2,5-Dihydroxy-1,4-benzoquinone

bttotb	H3bttotb = 4,4′,4″-(benzene-1,3,5-triyltris(oxy)) tribenzoicacid
atz	3-Amino-1,2,4-triazolate
ipa	Isophthalate
oba	4,4-Dicarboxyl diphenyl ether
tcpb	1,2,4,5-Tetrakis(4-carboxyphenyl)-benzene
NO_2ip	5-nitroisophthalate
dpe	1,2-Di(4-pyridyl)ethylene.

Conflicts of interest

The authors declare that they have no known competing financial interests or personal relationships that could have appeared to influence the work reported in this paper.

Acknowledgements

References

1 B. Li, X. Cui, D. O'Nolan, H.-M. Wen, M. Jiang, R. Krishna, H. Wu, R.-B. Lin, Y.-S. Chen, D. Yuan, H. Xing, W. Zhou, Q. Ren, G. Qian, M. J. Zaworotko and B. Chen, *Adv. Mater.*, 2017, **29**, 1704210.

2 D. Shi, X. Yu, W. Fan, V. Wee and D. Zhao, *Coord. Chem. Rev.*, 2021, **437**, 213794.

3 D. S. Sholl and R. P. Lively, *Nature*, 2016, **532**, 435–437.

4 K.-J. Chen, D. G. Madden, S. Mukherjee, T. Pham, K. A. Forrest, A. Kumar, B. Space, J. Kong, Q.-Y. Zhang and M. J. Zaworotko, *Science*, 2019, **366**, 241–246.

5 L. Li, R.-B. Lin, R. Krishna, X. Wang, B. Li, H. Wu, J. Li, W. Zhou and B. Chen, *J. Mater. Chem. A*, 2017, **5**, 18984–18988.

6 J. Wang, Q. Zhu, Z. Zhang, M. Sadakane, Y. Li and W. Ueda, *Angew. Chem., Int. Ed.*, 2021, **60**, 18328–18334.

7 M. Kang, S. Yoon, S. Ga, D. W. Kang, S. Han, J. H. Choe, H. Kim, D. W. Kim, Y. G. Chung and C. S. Hong, *Adv. Sci.*, 2021, **8**, 2004940.

8 T. Wang, E. Lin, Y.-L. Peng, Y. Chen, P. Cheng and Z. Zhang, *Coord. Chem. Rev.*, 2020, **423**, 213485.

9 P.-Q. Liao, W.-X. Zhang, J.-P. Zhang and X.-M. Chen, *Nat. Commun.*, 2015, **6**, 8697.

10 K. Su, W. Wang, S. Du, C. Ji and D. Yuan, *Nat. Commun.*, 2021, **12**, 3703.

11 L. Hashemi, M. Y. Masoomi and H. Garcia, *Coord. Chem. Rev.*, 2022, **472**, 214776.

12 L. Yang, S. Qian, X. Wang, X. Cui, B. Chen and H. Xing, *Chem. Soc. Rev.*, 2020, **49**, 5359–5406.

13 Y.-L. Peng, T. Pham, P. Li, T. Wang, Y. Chen, K.-J. Chen, K. A. Forrest, B. Space, P. Cheng, M. J. Zaworotko and Z. Zhang, *Angew. Chem., Int. Ed.*, 2018, **57**, 10971–10975.

14 Y. He, F. Chen, B. Li, G. Qian, W. Zhou and B. Chen, *Coord. Chem. Rev.*, 2018, **373**, 167–198.

15 R.-B. Lin, S. Xiang, H. Xing, W. Zhou and B. Chen, *Coord. Chem. Rev.*, 2019, **378**, 87–103.

16 W. Fan, S. Yuan, W. Wang, L. Feng, X. Liu, X. Zhang, X. Wang, Z. Kang, F. Dai, D. Yuan, D. Sun and H.-C. Zhou, *J. Am. Chem. Soc.*, 2020, **142**, 8728–8737.

17 W. Fan, X. Wang, X. Zhang, X. Liu, Y. Wang, Z. Kang, F. Dai, B. Xu, R. Wang and D. Sun, *ACS Cent. Sci.*, 2019, **5**, 1261–1268.

18 W. Fan, Y. Ying, S. B. Peh, H. Yuan, Z. Yang, Y. D. Yuan, D. Shi, X. Yu, C. Kang and D. Zhao, *J. Am. Chem. Soc.*, 2021, **143**, 17716–17723.

19 S. Yang, A. J. Ramirez-Cuesta, R. Newby, V. Garcia-Sakai, P. Manuel, S. K. Callear, S. I. Campbell, C. C. Tang and M. Schröder, *Nat. Chem.*, 2015, **7**, 121–129.

20 X. Jiang, T. Pham, J. W. Cao, K. A. Forrest, H. Wang, J. Chen, Q. Y. Zhang and K. J. Chen, *Chem. – Eur. J.*, 2021, **27**, 9446–9453.

21 X. Zhang, J.-X. Wang, L. Li, J. Pei, R. Krishna, H. Wu, W. Zhou, G. Qian, B. Chen and B. Li, *Angew. Chem., Int. Ed.*, 2021, **60**, 10304–10310.

22 H. Li, C. Liu, C. Chen, Z. Di, D. Yuan, J. Pang, W. Wei, M. Wu and M. Hong, *Angew. Chem., Int. Ed.*, 2021, **60**, 7547–7552.

23 Z. Di, C. Liu, J. Pang, C. Chen, F. Hu, D. Yuan, M. Wu and M. Hong, *Angew. Chem., Int. Ed.*, 2021, **60**, 10828–10832.

24 X. Li, H. Bian, W. Huang, B. Yan, X. Wang and B. Zhu, *Coord. Chem. Rev.*, 2022, **470**, 214714.

25 X. Cui, K. Chen, H. Xing, Q. Yang, R. Krishna, Z. Bao, H. Wu, W. Zhou, X. Dong, Y. Han, B. Li, Q. Ren, M. J. Zaworotko and B. Chen, *Science*, 2016, **353**, 141–144.

26 A. Cadiau, K. Adil, P. M. Bhatt, Y. Belmabkhout and M. Eddaoudi, *Science*, 2016, **353**, 137–140.

27 P.-Q. Liao, N.-Y. Huang, W.-X. Zhang, J.-P. Zhang and X.-M. Chen, *Science*, 2017, **356**, 1193–1196.

28 C. Gu, N. Hosono, J.-J. Zheng, Y. Sato, S. Kusaka, S. Sakaki and S. Kitagawa, *Science*, 2019, **363**, 387–391.

29 K. Adil, Y. Belmabkhout, R. S. Pillai, A. Cadiau, P. M. Bhatt, A. H. Assen, G. Maurin and M. Eddaoudi, *Chem. Soc. Rev.*, 2017, **46**, 3402–3430.

30 S. Mukherjee, D. Sensharma, K.-J. Chen and M. J. Zaworotko, *Chem. Commun.*, 2020, **56**, 10419–10441.

31 T. Lan, L. Li, Y. Chen, X. Wang, J. Yang and J. Li, *Mater. Chem. Front.*, 2020, **4**, 1954–1984.

32 W. Fan, X. Zhang, Z. Kang, X. Liu and D. Sun, *Coord. Chem. Rev.*, 2021, **443**, 213968.

33 E. D. Bloch, W. L. Queen, R. Krishna, J. M. Zadrozny, C. M. Brown and J. R. Long, *Science*, 2012, **335**, 1606–1610.

34 Q. Ding, Z. Zhang, P. Zhang, J. wang, X. Cui, C.-H. He, S. Deng and H. Xing, *Chem. Eng. J.*, 2022, **434**, 134784.

35 T. Loiseau, C. Serre, C. Huguenard, G. Fink, F. Taulelle, M. Henry, T. Bataille and G. Férey, *Chem. – Eur. J.*, 2004, **10**, 1373–1382.

36 S. K. Elsaidi, M. H. Mohamed, D. Banerjee and P. K. Thallapally, *Coord. Chem. Rev.*, 2018, **358**, 125–152.

37 A. Noonikara-Poyil, H. Cui, A. A. Yakovenko, P. W. Stephens, R.-B. Lin, B. Wang, B. Chen and H. V. R. Dias, *Angew. Chem., Int. Ed.*, 2021, **60**, 27184–27188.

38 Z. Bao, J. Wang, Z. Zhang, H. Xing, Q. Yang, Y. Yang, H. Wu, R. Krishna, W. Zhou, B. Chen and Q. Ren, *Angew. Chem., Int. Ed.*, 2018, **57**, 16020–16025.

39 X.-W. Gu, J.-X. Wang, E. Wu, H. Wu, W. Zhou, G. Qian, B. Chen and B. Li, *J. Am. Chem. Soc.*, 2022, **144**, 2614–2623.

40 S. Dutta, S. Mukherjee, O. T. Qazvini, A. K. Gupta, S. Sharma, D. Mahato, R. Babarao and S. K. Ghosh, *Angew. Chem., Int. Ed.*, 2022, **61**, e202114132.

41 Y. Wu and B. M. Weckhuysen, *Angew. Chem., Int. Ed.*, 2021, **60**, 18930–18949.

42 Z. Zhang, S. B. Peh, Y. Wang, C. Kang, W. Fan and D. Zhao, *Angew. Chem., Int. Ed.*, 2020, **59**, 18927–18932.

43 J. Wang, Y. Zhang, P. Zhang, J. Hu, R.-B. Lin, Q. Deng, Z. Zeng, H. Xing, S. Deng and B. Chen, *J. Am. Chem. Soc.*, 2020, **142**, 9744–9751.

44 J. Shen, X. He, T. Ke, R. Krishna, J. M. V. Baten, R. Chen, Z. Bao, H. Xing, M. Dinca, Z. Zhang, Q. Yang and Q. Ren, *Nat. Commun.*, 2020, **11**, 6259.

45 S. Geng, E. Lin, X. Li, W. Liu, T. Wang, Z. Wang, D. Sensharma, S. Darwish, Y. H. Andaloussi, T. Pham, P. Cheng, M. J. Zaworotko, Y. Chen and Z. Zhang, *J. Am. Chem. Soc.*, 2021, **143**, 8654–8660.

46 S.-Q. Yang and T.-L. Hu, *Coord. Chem. Rev.*, 2022, **468**, 214628.

47 R.-B. Lin, H. Wu, L. Li, X.-L. Tang, Z. Li, J. Gao, H. Cui, W. Zhou and B. Chen, *J. Am. Chem. Soc.*, 2018, **140**, 12940–12946.

48 H. Fang, B. Zheng, Z. H. Zhang, H. X. Li, D. X. Xue and J. Bai, *Angew. Chem., Int. Ed.*, 2021, **60**, 16521–16528.

49 B. Zhu, J.-W. Cao, S. Mukherjee, T. Pham, T. Zhang, T. Wang, X. Jiang, K. A. Forrest, M. J. Zaworotko and K.-J. Chen, *J. Am. Chem. Soc.*, 2021, **143**, 1485–1492.

50 Y. Wang, C. Hao, W. Fan, M. Fu, X. Wang, Z. Wang, L. Zhu, Y. Li, X. Lu, F. Dai, Z. Kang, R. Wang, W. Guo, S. Hu and D. Sun, *Angew. Chem., Int. Ed.*, 2021, **60**, 11350–11358.

51 Y. Wang, M. Fu, S. Zhou, H. Liu, X. Wang, W. Fan, Z. Liu, Z. Wang, D. Li, H. Hao, X. Lu, S. Hu and D. Sun, *Chem*, 2022, **8**, 3263–3274.

52 S.-Q. Yang, F.-Z. Sun, P. Liu, L. Li, R. Krishna, Y.-H. Zhang, Q. Li, L. Zhou and T.-L. Hu, *ACS Appl. Mater. Interfaces*, 2021, **13**, 962–969.

53 H.-G. Hao, Y.-F. Zhao, D.-M. Chen, J.-M. Yu, K. Tan, S. Ma, Y. Chabal, Z.-M. Zhang, J.-M. Dou, Z.-H. Xiao, G. Day, H.-C. Zhou and T.-B. Lu, *Angew. Chem., Int. Ed.*, 2018, **57**, 16067–16071.

54 Z. Xu, X. Xiong, J. Xiong, R. Krishna, L. Li, Y. Fan, F. Luo and B. Chen, *Nat. Commun.*, 2020, **11**, 3163.

55 H. M. Wen, C. Yu, M. Liu, C. Lin, B. Zhao, H. Wu, W. Zhou, B. Chen and J. Hu, *Angew. Chem., Int. Ed.*, 2023, **62**, e202309108.

56 Y.-Y. Xiong, C.-X. Chen, T. Pham, Z.-W. Wei, K. A. Forrest, M. Pan and C.-Y. Su, *CCS Chem.*, 2024, **6**, 241–254.

57 Q. Ding, Z. Zhang, Y. Liu, K. Chai, R. Krishna and S. Zhang, *Angew. Chem., Int. Ed.*, 2022, **61**, e202208134.

58 G.-D. Wang, Y.-Z. Li, W.-J. Shi, L. Hou, Y.-Y. Wang and Z. Zhu, *Angew. Chem., Int. Ed.*, 2022, **61**, e202205427.

59 R. Krishna, *ACS Omega*, 2020, **5**, 16987–17004.

60 Z. Chang, D.-H. Yang, J. Xu, T.-L. Hu and X.-H. Bu, *Adv. Mater.*, 2015, **27**, 5432–5441.

61 S. Krause, N. Hosono and S. Kitagawa, *Angew. Chem., Int. Ed.*, 2020, **59**, 15325–15341.

62 J. Y. Kim, J. Park, J. Ha, M. Jung, D. Wallacher, A. Franz, R. Balderas-Xicohténcatl, M. Hirscher, S. G. Kang, J. T. Park, I. H. Oh, H. R. Moon and H. Oh, *J. Am. Chem. Soc.*, 2020, **142**, 13278–13282.

63 M. Bonneau, C. Lavenn, J.-J. Zheng, A. Legrand, T. Ogawa, K. Sugimoto, F.-X. Coudert, R. Reau, S. Sakaki, K.-I. Otake and S. Kitagawa, *Nat. Chem.*, 2022, **14**, 816–822.

64 S. Horike, S. Shimomura and S. Kitagawa, *Nat. Chem.*, 2009, **1**, 695–704.

65 Q. Dong, X. Zhang, S. Liu, R.-B. Lin, Y. Guo, Y. Ma, A. Yonezu, R. Krishna, G. Liu, J. Duan, R. Matsuda, W. Jin and B. Chen, *Angew. Chem., Int. Ed.*, 2020, **59**, 22756–22762.

66 Q. Dong, Y. Huang, K. Hyeon-Deuk, I.-Y. Chang, J. Wan, C. Chen, J. Duan, W. Jin and S. Kitagawa, *Adv. Funct. Mater.*, 2022, **32**, 2203745.

67 S. Mukherjee, N. Kumar, A. A. Bezrukov, K. Tan, T. Pham, K. A. Forrest, K. A. Oyekan, O. T. Qazvini, D. G. Madden, B. Space and M. J. Zaworotko, *Angew. Chem., Int. Ed.*, 2021, **60**, 10902–10909.

68 Y. Jiang, Y. Hu, B. Luan, L. Wang, R. Krishna, H. Ni, X. Hu and Y. Zhang, *Nat. Commun.*, 2023, **14**, 401.

69 T. Ke, Q. Wang, J. Shen, J. Zhou, Z. Bao, Q. Yang and Q. Ren, *Angew. Chem., Int. Ed.*, 2020, **59**, 12725–12730.

70 L. Li, H.-M. Wen, C. He, R.-B. Lin, R. Krishna, H. Wu, W. Zhou, J. Li, B. Li and B. Chen, *Angew. Chem., Int. Ed.*, 2018, **57**, 15183–15188.

71 P. Nugent, Y. Belmabkhout, S. D. Burd, A. J. Cairns, R. Luebke, K. Forrest, T. Pham, S. Ma, B. Space, L. Wojtas, M. Eddaoudi and M. J. Zaworotko, *Nature*, 2013, **495**, 80–84.

72 J.-W. Cao, S. Mukherjee, T. Pham, Y. Wang, T. Wang, T. Zhang, X. Jiang, H.-J. Tang, K. A. Forrest, B. Space, M. J. Zaworotko and K.-J. Chen, *Nat. Commun.*, 2021, **12**, 6507.

73 Chemicals & Resources. Chemical Industry. Production capacity of propylene worldwide in 2018 and 2030. **https://www.statista.com/statistics/1065879/global-propylene-production-capacity/**.

74 H. Zeng, M. Xie, T. Wang, R.-J. Wei, X.-J. Xie, Y. Zhao, W. Lu and D. Li, *Nature*, 2021, **595**, 542–548.

75 S.-Q. Yang, F.-Z. Sun, R. Krishna, Q. Zhang, L. Zhou, Y.-H. Zhang and T.-L. Hu, *ACS Appl. Mater. Interfaces*, 2021, **13**, 35990–35996.

76 A. N. Hong, H. Yang, T. Li, Y. Wang, Y. Wang, X. Jia, A. Zhou, E. Kusumoputro, J. Li, X. Bu and P. Feng, *ACS Appl. Mater. Interfaces*, 2021, **13**, 52160–52166.

77 Y.-L. Peng, T. Wang, C. Jin, C.-H. Deng, Y. Zhao, W. Liu, K. A. Forrest, R. Krishna, Y. Chen, T. Pham, B. Space, P. Cheng, M. J. Zaworotko and Z. Zhang, *Nat. Commun.*, 2021, **12**, 5768.

78 P. Zhang, L. Yang, X. Liu, J. Wang, X. Suo, L. Chen, X. Cui and H. Xing, *Nat. Commun.*, 2022, **13**, 4928.

79 J. Li, X. Han, X. Kang, Y. Chen, S. Xu, G. L. Smith, E. Tillotson, Y. Cheng, L. J. McCormick McPherson, S. J. Teat, S. Rudic, A. J. Ramirez-Cuesta, S. J. Haigh, M. Schroder and S. Yang, *Angew. Chem., Int. Ed.*, 2021, **60**, 15541–15547.

80 B. Liang, X. Zhang, Y. Xie, R.-B. Lin, R. Krishna, H. Cui, Z. Li, Y. Shi, H. Wu, W. Zhou and B. Chen, *J. Am. Chem. Soc.*, 2020, **142**, 17795–17801.

81 L. Yu, X. Han, H. Wang, S. Ullah, Q. Xia, W. Li, J. Li, I. D. Silva, P. Manuel, S. Rudić, Y. Cheng, S. Yang, T. Thonhauser and J. Li, *J. Am. Chem. Soc.*, 2021, **143**, 19300–19305.

82 J. Gao, Y. Cai, X. Qian, P. Liu, H. Wu, W. Zhou, D.-X. Liu, L. Li, R.-B. Lin and B. Chen, *Angew. Chem., Int. Ed.*, 2021, **60**, 20400–20406.

83 L. Li, L. Guo, F. Zheng, Z. Zhang, Q. Yang, Y. Yang, Q. Ren and Z. Bao, *ACS Appl. Mater. Interfaces*, 2020, **12**, 17147–17154.

84 L. Yang, X. Cui, Z. Zhang, Q. Yang, Z. Bao, Q. Ren and H. Xing, *Angew. Chem., Int. Ed.*, 2018, **57**, 13145–13149.

85 Z. Zhang, Q. Ding, J. Cui, X. Cui and H. Xing, *Small*, 2020, **16**, 2005360.

86 Q. Wang, J. Hu, L. Yang, Z. Zhang, T. Ke, X. Cui and H. Xing, *Nat. Commun.*, 2022, **13**, 2955.

87 P. Hu, J. Hu, H. Liu, H. Wang, J. Zhou, R. Krishna and H. Ji, *ACS Cent. Sci.*, 2022, **8**, 1159–1168.

88 J. Cui, Z. Zhang, J. Hu, L. Yang, Y. Li, L. Chen, X. Cui and H. Xing, *Chem. Eng. J.*, 2021, **425**, 130580.

89 B. R. Barnett, S. T. Parker, M. V. Paley, M. I. Gonzalez, N. Biggins, J. Oktawiec and J. R. Long, *J. Am. Chem. Soc.*, 2019, **141**, 18325–18333.

90 A. H. Assen, Y. Belmabkhout, K. Adil, P. M. Bhatt, D.-X. Xue, H. Jiang and M. Eddaoudi, *Angew. Chem., Int. Ed.*, 2015, **54**, 14353–14358.

91 P.-Q. Liao, N.-Y. Huang, W.-X. Zhang, J.-P. Zhang and X.-M. Chen, *Science*, 2017, **356**, 1193–1196.

92 P.-Q. Liao, D.-D. Zhou, A.-X. Zhu, L. Jiang, R.-B. Lin, J.-P. Zhang and X.-M. Chen, *J. Am. Chem. Soc.*, 2012, **134**, 17380–17383.

93 Z. Zhang, Q. Yang, X. Cui, L. Yang, Z. Bao, Q. Ren and H. Xing, *Angew. Chem., Int. Ed.*, 2017, **56**, 16282–16287.

94 J. Chen, J. Wang, L. Guo, L. Li, Q. Yang, Z. Zhang, Y. Yang, Z. Bao and Q. Ren, *ACS Appl. Mater. Interfaces*, 2020, **12**, 9609–9616.

95 K. Kishida, Y. Okumura, Y. Watanabe, M. Mukoyoshi, S. Bracco, A. Comotti, P. Sozzani, S. Horike and S. Kitagawa, *Angew. Chem., Int. Ed.*, 2016, **55**, 13784–13788.

96 Z. Zhang, S. B. Peh, C. Kang, K. Chai and D. Zhao, *EnergyChem*, 2021, **3**, 100057.

97 Y. Yu, L. Yang, B. Tan, J. Hu, Q. Wang, X. Cui and H. Xing, *Nano Res.*, 2021, **14**, 541–545.

98 P. S. Bárcia, F. Zapata, J. A. C. Silva, A. E. Rodrigues and B. Chen, *J. Phys. Chem. B*, 2007, **111**, 6101–6103.

99 Z. R. Herm, B. M. Wiers, J. A. Mason, J. M. V. Baten, M. R. Hudson, P. Zajdel, C. M. Brown, N. Masciocchi, R. Krishna and J. R. Long, *Science*, 2013, **340**, 960–964.

100 L. Yu, X. Dong, Q. Gong, S. R. Acharya, Y. Lin, H. Wang, Y. Han, T. Thonhauser and J. Li, *J. Am. Chem. Soc.*, 2020, **142**, 6925–6929.

101 H. Wang, X. Dong, E. Velasco, D. H. Olson, Y. Han and J. Li, *Energy Environ. Sci.*, 2018, **11**, 1226–1231.

102 H. Wang, X. Dong, J. Lin, S. J. Teat, S. Jensen, J. Cure, E. V. Alexandrov, Q. Xia, K. Tan, Q. Wang, D. H. Olson, D. M. Proserpio, Y. J. Chabal, T. Thonhauser, J. Sun, Y. Han and J. Li, *Nat. Commun.*, 2018, **9**, 1745.

103 H. Zhao, G. Maurin and A. Ghoufi, *J. Chem. Phys.*, 2021, **154**, 084702.

104 R. Krishna, *Phys. Chem. Chem. Phys.*, 2015, **17**, 39–59.

105 R. Krishna, *Sep. Purif. Technol.*, 2019, **215**, 227–241.

106 D. Dubbeldam, R. Krishna, S. Calero and A. O. Yazaydin, *Angew. Chem., Int. Ed.*, 2012, **51**, 11867–11871.

107 B. Smit and T. L. M. Maesen, *Nature*, 1995, **374**, 42–44.

108 J. Talbot, *AIChE J.*, 1997, **43**, 2471–2478.

109 Z. Du, G. Manos, T. J. H. Vlugt and B. Smit, *AIChE J.*, 1998, **44**, 1756–1764.

110 J. M. van Baten and R. Krishna, *Microporous Mesoporous Mater.*, 2005, **84**, 179–191.

111 R. Krishna, B. Smit and S. Calero, *Chem. Soc. Rev.*, 2002, **31**, 185–194.

112 R. Krishna and J. M. V. Baten, *Phys. Chem. Chem. Phys.*, 2011, **13**, 10593–10616.

113 A. Torres-Knoop, R. Krishna and D. Dubbeldam, *Angew. Chem., Int. Ed.*, 2014, **53**, 7774–7778.

114 A. Torres-Knoop, S. R. Balestra, R. Krishna, S. Calero and D. Dubbeldam, *Chem. Phys. Chem.*, 2015, **16**, 532–535.

115 A. Torres-Knoop and D. Dubbeldam, *ChemPhysChem*, 2015, **16**, 2046–2067.

116 R. Krishna, *RSC Adv.*, 2015, **5**, 52269–52295.

117 R. Krishna, *RSC Adv.*, 2017, **7**, 35724–35737.

118 R. Krishna, *Sep. Purif. Technol.*, 2018, **194**, 281–300.

119 Y. Yang, P. Bai and X. Guo, *Ind. Eng. Chem. Res.*, 2017, **56**, 14725–14753.

120 V. Finsy, H. Verelst, L. Alaerts, D. D. Vos, P. A. Jacobs, G. V. Baron and J. F. M. Denayer, *J. Am. Chem. Soc.*, 2008, **130**, 7110–7118.

121 F. Vermoortele, M. Maes, P. Z. Moghadam, M. J. Lennox, F. Ragon, M. Boulhout, S. Biswas, K. G. M. Laurier, I. Beurroies, R. Denoyel, M. Roeffaers, N. Stock, T. Duren, C. Serre and D. E. D. Vos, *J. Am. Chem. Soc.*, 2011, **133**, 18526–18529.

122 M. I. Gonzalez, M. T. Kapelewski, E. D. Bloch, P. J. Milner, D. A. Reed, M. R. Hudson, J. A. Mason, G. Barin, C. M. Brown and J. R. Long, *J. Am. Chem. Soc.*, 2018, **140**, 3412–3422.

123 X. Cui, Z. Niu, C. Shan, L. Yang, J. Hu, Q. Wang, P. C. Lan, Y. Li, L. Wojtas, S. Ma and H. Xing, *Nat. Commun.*, 2020, **11**, 5456.

124 A. A. Sapianik, E. R. Dudko, K. A. Kovalenko, M. O. Barsukova, D. G. Samsonenko, D. N. Dybtsev and V. P. Fedin, *ACS Appl. Mater. Interfaces*, 2021, **13**, 14768–14777.

125 K. B. Idrees, Z. Li, H. Xie, K. O. Kirlikovali, M. Kazem-Rostami, X. Wang, X. Wang, T.-Y. Tai, T. Islamoglu, J. F. Stoddart, R. Q. Snurr and O. K. Farha, *J. Am. Chem. Soc.*, 2022, **144**, 12212–12218.

126 L. Li, L. Guo, D. H. Olson, S. Xian, Z. Zhang, Q. Yang, K. Wu, Y. Yang, Z. Bao, Q. Ren and J. Li, *Science*, 2022, **377**, 335–339.

127 S. Mukherjee, A. V. Desai and S. K. Ghosh, *Coord. Chem. Rev.*, 2018, **367**, 82–126.

128 S. Mukherjee, B. Joarder, B. Manna, A. V. Desai, A. K. Chaudhari and S. K. Ghosh, *Sci. Rep.*, 2014, **4**, 5761.

129 S.-Q. Wang, S. Mukherjee, E. Patyk-Kaźmierczak, S. Darwish, A. Bajpai, Q.-Y. Yang and M. J. Zaworotko, *Angew. Chem., Int. Ed.*, 2019, **58**, 6630–6634.

130 D.-D. Zhou, P. Chen, C. Wang, S.-S. Wang, Y. Du, H. Yan, Z.-M. Ye, C.-T. He, R.-K. Huang, Z.-W. Mo, N.-Y. Huang and J.-P. Zhang, *Nat. Mater.*, 2019, **18**, 994–998.

131 S. M. Vornholt and R. E. Morris, *Nat. Mater.*, 2019, **18**, 910–911.

132 A. Torres-Knoop, J. Heinen, R. Krishna and D. Dubbeldam, *Langmuir*, 2015, **31**, 3771–3778.

133 M. Lusi and L. J. Barbour, *Chem. Commun.*, 2013, **49**, 2634–2636.

134 A. M. Kałuża, S. Mukherjee, S.-Q. Wang, D. J. O'Hearn and M. J. Zaworotko, *Chem. Commun.*, 2020, **56**, 1940–1943.